UPTEC X 07 040
Examensarbete 20 p
Augusti 2007

Characterization of possible oncofetal antigens in lung cancer applying antibody library

J. Peter Johansson

UPPSALA UNIVERSITET

Molecular Biotechnology Programme

Uppsala University School of Engineering

UPTEC X 07 040	**Date of issue 2007-08**

Author

J. Peter Johansson

Title (English)

Characterization of possible oncofetal antigens in lung cancer applying antibody library

Abstract

Emryogenesis, the development of an embryo, and oncogenesis, the formation of a tumor, are both driven by unique self-renewing stem cells. Tumor markers present during these two processes are called oncofetal antigens. In this work a library of antibodies, raised mainly against human embryonic stem cells, has been screened for oncofetal antigens displayed by lung cancer cells. Characterization was performed employing CELISA, western blotting, immunocytochemistry, periodate sensitivity measurements and phage display. A number of antigens, possibly of oncofetal nature, have been described. Multiple antigens were proven to be secreted and therefore applicable as tumor markers. Also, an antigen maybe exclusively present in adenocarcinomas was found.

Keywords

Oncofetal antigen, antibody library, human embryonal stem cell, tumor marker, CELISA, western blotting, immunocytochemistry, phage display

Supervisors

Christian Fermér
Fujirebio Diagnostics AB, Gothenburg

Scientific reviewer

Ingela Turesson
Department of Oncology, Rudbeck Laboratory, Uppsala

Project name	Sponsors
Language **English**	Security
ISSN 1401-2138	Classification
Supplementary bibliographical information	Pages **49**

Biology Education Centre Biomedical Center Husargatan 3 Uppsala
Box 592 S-75124 Uppsala Tel +46 (0)18 4710000 Fax +46 (0)18 555217

Characterization of possible oncofetal antigens in lung cancer applying antibody library

J. Peter Johansson

Sammanfattning

Utvecklingen av ett foster samt bildandet av en tumör kännetecknas båda av celltillväxt. De kemiska substanser som endast förekommer vid dessa två processer kallas oncofetala och kan användas som tumörmarkörer vid diagnostisering, prognostisering och monitorering av cancer. Idag tillämpas ett antal oncofetala antigen som tumörmarkörer rutinmässigt i sjukvården, exempelvis carcinoembryonic antigen praktiseras vid monitorering av patienter med diagnostiserad colorektal cancer för att upptäcka eventuella levermetastaser tidigt. Genom att använda speciellt framtagna antikroppar kan man kontinuerligt fastställa mängden oncofetala substanser i ett blodprov och på så sätt bland annat följa cancerbehandlingens fortskridande.

De applicerade antikropparna framställs genom att man injicerar en mus med en främmande enhet varpå musen bildar antikroppar mot denna. Innan projektet startades hade ett antal möss injicerats med till mestadels humana embryonal stamceller, vilka förekommer vid utvecklingen av ett embryo. Detta resulterade i ett bibliotek av antikroppar, som använts under arbetet för att försöka finna oncofetala antigen uttryckta av främst lungcancerceller. Under projektet har ett antal möjliga oncofetala antigen karakteriserat genom att applicera några välkända molekylärbiologiska tekniker. Ett flertal antigen har bevisats utsöndras av cancerceller, vilket gör dem tillämpliga som tumörmarkörer. Dessutom hittades ett antigen som möjligtvis uttrycks exklusivt av adenocarcinom.

Examensarbete 20 p i Molekylär bioteknikprogrammet

Uppsala universitet, augusti 2007

Contents

1 Background and aim

This Master of Science project has been performed at Fujirebio Diagnostics (Gothenburg, Sweden) and is one part of an ongoing project conducted in a partnership between Fujirebio Diagnostics and Cellartis (Gothenburg, Sweden). Both companies contribute to the project with their respective knowledge: establishment of monoclonal antibodies (Fujirebio Diagnostics) and growth/cultivation of human embryonic stem (hES) cells (Cellartis). The complete project has two aims, a primary aim of establishing monoclonal antibodies against antigens exclusively present on undifferentiated hES cells, and a secondary aim of establishing monoclonal antibodies specific for early differentiated hES cells (e.g. human progenitor stem cells).

This thesis work has aimed at identifying oncofetal antigens in lung cancer applying an antibody library raised against mainly hES cells and early differentiated cells. Hopefully, the identification of oncofetal antigens might lead to development of effective cancer diagnostic, prognosis and monitoring tools.

2 Abbreviations

AFP α-fetoprotein
AML acute myeloid leukemia
AT2 alveolar type 2
BADJ bronchoalveolar duct junction
BSA bovine serum albumin
CA cancer antigen
CEA carcinoembryonic antigen
CELISA cell enzyme linked immunosorbent assay
CSC cancer stem cell
CTC circulating metastatic cell
DMEM dulbecco's modified eagle medium
DTT dithiothreitol
EB embryoid bodies
EDTA ethylenediaminetetraacetic acid
FBS fetal bovine serum
FITC fluoresceinisotiocyanat
hEC human embryonal carcinoma
hES human embryonic stem
HRP horseradish peroxidase
HSC haematopoietic stem cells
HT hypoxanthine thymidine
ICC immunocytochemistry
ICM inner cell mass
IMDM icove's modified dulbecco's medium.
Oct4 octamer-binding transcription factor-4
ON over night
OPD o-phenylenediamine dihydrochloride
NEB neuroepithelial body
PBS phosphate buffered saline
PEG poly ethylene glycol
PFA paraformaldehyde
PLL poly-l-lysine
PMSF phenylmethylsulphonyl fluoride
PNEC pulmonary neuroendocrine cell
PSA prostate specific antigen
RT room temperature
SCC squamous cell carcinoma
SCLC small cell lung carcinoma
SHH sonic hedgehog
SSEA stage-specfic embryonic antigen
TA transit amplifying
TBS tris buffered saline
TRA tumor rejection antigen
TRIS trishydroxymethylaminomethane

3 Introduction

The introduction will firstly explain the concepts and clinical applications of tumor markers. Thereafter, stem cells are defined and parallels between adult stem cells, embryonic stem cells and embryonal carcinoma cells are drawn indicating a link between embryogenesis and oncogenesis resulting in cancer stem cell theory. Finally, proofs of lung stem cells and lung cancer stem cells will be explored.

3.1 Tumor markers – valuable tools in cancer monitoring

A tumor marker can be defined as a biochemical substance produced by a tumor or by the body in response to a tumor in a higher than normal amount detectable in cancer diagnostics. In practice, most tumor markers are proteins or glycoproteins tested in serum. The ideal tumor marker is: (i) exclusively secreted from malignant or premalignant tissue highly plausible to persist into malignancy; (ii) displayed in significantly heightened amounts in a tumor specific manner in all patients; (iii) produced organ-specifically; (iv) easily detected and measured in an easily obtainable body fluid (e.g. serum) at a premalignant phase or during initial malignancy; (v) expressed in an amount proportional to tumor status (e.g. concentration proportional to tumor volume or tumor future biological behavior); (vi) demonstrating a relatively short half-life enabling quick indications of therapy; (vii) applicable in simple, cheap, standardized and reproducible assays. [1]

None of the presently utilized tumor markers possess all these practical features, but display disadvantages. The most commonly addressed limitations are: (i) incapability, regarding some tumor markers, to separate malignant and benign (i.e. deficit of specificity) disorders (e.g. prostate specific antigen (PSA) measurable in elevated amounts in both benign hypertrophy of the prostate and prostate carcinoma); (ii) failure to detect early malignancy (i.e. deficit of sensitivity) in patients (e.g. elevated amounts of cancer antigen (CA) 15-3 only found in patients with advanced breast cancer); (iii) heightened levels of tumor markers with a specific tumor sort are only exhibited by a subpopulation of all patients; (iv) no completely organ specific tumor marker (e.g. CA 19-9 elevated in most advanced adenocarcinoma patients), apart from PSA, expressing nearly prostate specific properties. [1]

Tumor markers could be or are applied in: (i) screening, performed in a large systematic survey of seemingly healthy individuals to detect cancer prior to symptoms are displayed; (ii) diagnosis, used to establish symptoms origin and start treatment if malignancy is detected, that is, testing patients experiencing symptoms related to cancer; (iii) prognosis and prediction of therapy responses, employed to optimize therapy in order to avoid undertreatment regarding aggressive disease or overtreatment regarding indolent disease; (iv) monitoring, applied to discover reappearance of malignancy and observe advanced disease. Monitoring is the main application of most tumor markers today. [1]

3.1.1 Oncofetal antigens – commonly employed tumor markers

An oncofetal antigen can be defined as: “A tumor marker produced by tumor tissue and by fetal tissue of the same type as the tumor, but not by normal adult tissue from which the tumor arises” [2]. During events associated with cell proliferation and differentiation, such as fetus development and malignancy, oncofetal antigens are produced in high concentrations. In malignancy, oncofetal antigens work to suppress host immune system, inhibiting the cellular immunity, causing host to become tolerant to abnormal cells [3]. A number of tumor markers

of oncofetal feature are today utilized routinely [4]. Here three of them will be introduced in short: α-fetoprotein (AFP), cancer antigen 125 (CA 125) and carcinoembryonic antigen (CEA). Alfa-fetprotein, a single-chain polypeptide, is a 70 kDa glycoprotein [3]. AFP, introduced as a tumor marker in the 1970s, is relatively specific for hepatocellular carcinoma and nonseminomatous germ cell tumors and is therefore used in screening, prognosing and monitoring [4]. CA 125 is a non-mucinoid (i.e. not a glycoprotein secreted by mucous membranes) glycoprotein of molecular weight higher than 200 kDa. In the circulation CA 125 molecules form complexes with molecular weights exceeding 1000 kDa [3]. CA 125 was introduced in the 1980s and routinely used for monitoring non-mucinos ovarian cancer [4]. Carcinoembryonic antigen, a glycoprotein of 180 kDa molecular weight, consists of approximately 40% protein and 60% carbohydrate [3]. CEA was introduced during the 1970s and is today utilized in monitoring patients with diagnosed colorectal cancer, primarily for its sensitivity in detecting liver metastasis [4].

3.2 Stem cells and embryogenesis – basis of the multicellular organism

Stem cells are defined as cells capable of self-renewing, implying the potential to produce at least one unaltered daughter cell following cell division with the capacity for differentiation. The potency of a cell is limited by the available range of commitment as seen in Table 1. [5]

During embryonic development a predetermined path is accompanied by loss of potency as cells become more differentiated [6]. When the zygote starts to divide totipotency is lost and the formation of an embryo is initiated. Embryogenesis are roughly divided into three distinct stages: morula stage, formation of a ball of cells, blastocyst stage, development of a cavity, and gastrula stage, differentiation into the three primary germ layers of cells, called endoderm, ectoderm and mesoderm, that subsequently will generate all the cell types of the body and ultimately give rise to all the specialized tissues and organs of a complete organism. The ectoderm develops into skin and nervous system. The mesoderm generates muscle, blood, bone and fat. The endoderm gives rise to the gut, liver, pancreas, and lungs [7]. Posterior of gastrulation, the only pluripotent cells remaining in the embryo are the germ cells [6].

Table 1. The potency of cells [5]

Potency	Description	Example
Totipotent	Able to form entire organism	Zygote
Pluripotent	Able to form all the body's lineages	Embryonic stem cell
Multipotent	Able to form multiple lineages that constitute an entire tissue or tissues	Haematopoietic stem cell
Oligopotent	Able to form two or more lineages within a tissue	Neural stem cell creating a subset of neurons in the brain
Unipotent	Able to form a single lineage within a tissue	Spermatogonial stem cell

3.3 Human adult stem cells – tissue specific stem cells

It has been shown that many tissues and organs in the mature organism contain small populations of undifferentiated cells among differentiated cells. These cells do not show pluripotency, but display multipotent/oligopotent stem cell characteristics and are called adult stem cells (i.e. somatic stem cells). The adult stem cells are thought to be localized at distinct parts of tissues and organs, commonly known as "niches", regulating their fate. Here they can remain quiescent, non dividing, for years [8]. Adult stem cells serve as long term reservoirs generating populations of daughter cells, called transit amplifying (TA) cells, displaying

potentials to proliferate at high rate, to self-renew in the short term and to produce precursors capable of differentiating to all or many cell types of the organ (see Figure 1) [9]. Today it is believed that most tissues contain adult stem cells [9]. Somatic stem cells have been reported in brain, bone marrow, peripheral blood, blood vessels, skeletal muscle, skin, and liver and are believed to participate in tissue reparation and during maintenance of the tissue within they are located [8]. The adult stem cells are possibly an important participant in oncogenesis and cancer relapses. This feature will be further addressed when a short summary of cancer stem cell theory is presented later.

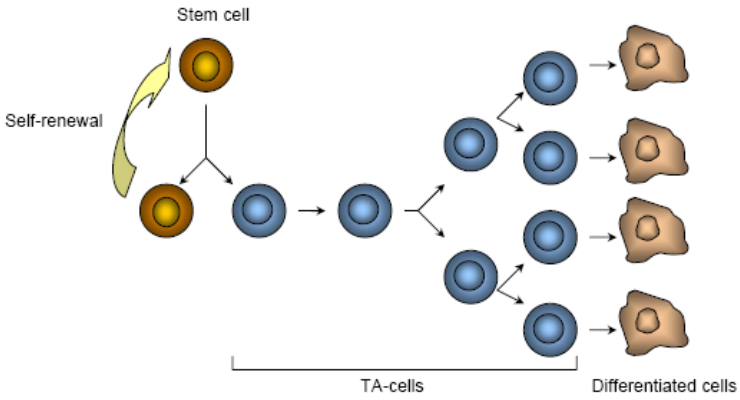

Figure 1. A stem cell can self-renew by asymmetric cell division also producing a TA-cell. TA-cells commonly proliferate prior to differentiation. Illustration adapted from [9].

3.4 Human embryonic stem cells – pluripotent stem cells

Human embryonic stem (hES) cells were first derived by Thomson *et al* in 1998 using fresh or frozen cleavage stage human embryos produced by *in vitro* fertilization for clinical purposes. Isolating 14 cells from the inner cell mass (ICM) of blastocyst stage embryos resulted in five hES cell lines originating from five distinct embryos (see Figure 2).[10]

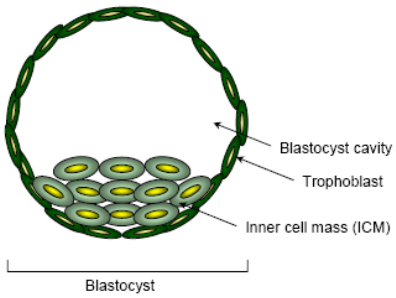

Figure 2. hES cells are isolated from the inner cell mass of blastocyst stage embryos.

Defining hES cells, the basic stem cell definition is prolonged by the ability of acting in a pluripotent way. To asses the pluripotent potential of hES cells, one of the following two methods are applied: (i) hES cells are injected (subcutaneously or intramuscularly) into immunocompromised mice and if a tumor, containing endoderm, mesoderm and ectoderm cell types, forms in 3-4 months this indicates the pluripotent nature of the hES cells; (ii) hES cells are maintained in suspension and aggregates of differentiated cells, called “embryoid bodies” (EBs), are generated and allowed to grow for 4 or more days. Plating is followed and further differentiation is accomplished. Colonies displaying differentiated cells of endoderm, mesoderm and ectoderm types originate by definition from pluripotent hES cells. [11]

When defining hES cells, they are regarded as self-renewing and pluripotent cells with the following characteristics: (i) can be isolated from the ICM; (ii) proliferate extensively *in vitro*; (iii) maintain a normal euploid karyotype over extended culture; (iv) differentiate into derivatives of all three germ layers; (v) express high levels of the octamer-binding transcription factor-4 (Oct4) and (vi) show telomerase activity. [12]

hES cells are often characterized applying a set of components associated with undifferentiated cells including the expression of surface markers and transcription factors. Commonly employed cell surface markers include diverse glycoproteins, such as tumor rejection antigen-1-60 (TRA-1-60) and tumor rejection antigen-1-81 (TRA-1-81), and glycolipids, such as stage-specfic embryonic antigen-3 (SSEA-3) and stage-specfic embryonic antigen-4 (SSEA-4), all originally identified as markers specific for human embryonal carcinoma (hEC) cells (described later). The maintenance of stem cell self-renewal is controlled by numerous transcription factors and expression analysis of these factors is also utilized to characterize hES cells. Oct3/4, one of those factors and belonging to the POU family of transcriptional regulators, is expressed both *in vivo* and *in vitro* cultures of pluripotent cell populations. Downregulation of Oct3/4 is seen upon cellular differentiation. Multiple studies have shown cell surface markers and expression patterns, characteristic of pluripotent stem cells, to be maintained in long-term cultures of hES cells. [12]

3.5 Human embryonal carcinoma cells – the first pluripotent cells studied

The first pluripotent cells were isolated in the early 1970s from tumors usually arising from germ cells called teratocarcinomas [11]. Teratocarcinomas are composed of teratoma cells and EC cells. A teratoma tumor contains a mixture of differentiated somatic cells and can display well distinguishable anatomical structures such as nerve, bone and muscle tissue. The EC cells act as pluripotent reservoirs and have been proven to serve as the malignant stem cell component of these tumors. Transplanting a single EC cell from one tumor into a new host generated a new teratocarcinoma filled with differentiate cells as observed in the parental tumor. [13]

EC cells are undifferentiated epithelial cells displaying features common with embryonic cells of the ICM such as SSEA-3, SSES-4, TRA-1-60 and TRA-1-81 [14]. Also typical for EC-cells is the expression of the gene POU5F1 encoding Oct-4 [15] and the formation of embryoid bodies when forced to grow in suspension [13]. As described earlier all these features are seen in culturing of hES cells.

The thesis of EC cells acting as a caricature of undifferentiated stem cells from the early embryo, during teratocarcinoma development, were tested by transmitting a few EC cells from teratocarcinomas of agouti mouse into a blastocyst of an albino mouse and thereafter re-implanting blastocysts into pseudopregnant females. Offspring exhibited parental characteristics from both EC cells and original blastocysts, namely a combination of albino and agouti fur. Later, similar experiments indicated implanted EC cells being responsible for almost all tissue generated in the host embryo. These results presented a resemblance of EC cells to cells of ICM and also demonstrated the malignant nature of EC cells being suppressed when merged with the embryo. The results were in favor of the ideas that the differentiated offspring cells of EC cells are generally not malignant. Thus indicating cancer formation, and not only that of teratocarcinomas, being related to deficiencies in the normal control mechanisms of stem cell differentiation. [13]

3.6 Cancer stem cells – theory of driving force behind cancer malignancy

Nowadays, the concept of a small subpopulation, displaying self-renewal features, with a great tumorigenic capability is in large excepted. In 1855 Rudolph Virchow formulated the first ideas of what today is known as cancer stem cell theory, when he discovered parallels between tumor development and tissue generation. Observing histological resemblances between the developing fetus and cancers (e.g. embryocarcinomas), he proposed his "embryonal-rest hypothesis" of cancer, suggesting tumor formation to be generated from dormant remaining embryonic tissue. [16]

For a long time, similarities between cancer cells and somatic stem cells have been observed. Both types of cells self-renew, although somatic stem cells renew in a highly regulated manner, whereas cancer cells renew in an uncontrolled way. Therefore it has been hypothesized that multiple signaling pathways employed in somatic stem cell self-renewal might be active in a dysregulated manner in neoplastic proliferation. This has been shown in WNT, sonic hedgehog (SHH), Notch, PTEN and BMI1 pathways. Moreover, both types of cells are capable of differentiation, but somatic stem cells create normal mature cells, whereas cancer cells often generate abnormal cells. [17]

The cancer stem cell theory suggests viewing a tumor as an abnormal organ initiated by a tumorigenic malignant cancer cell, the cancer stem cell (CSC). By applying the principles of stem cell biology to tumorigenesis, cells of the tumor can be organized into a hierarchical system where they are phenotypically different and hold separate proliferative capacities. Defining the cancer stem cell, a potential of transferring disease or form tumors when transplanted is addressed to the cancer cell. Furthermore, a cancer stem cell has a potential to perform self-renewal, generating additional tumorigenic cancer cells of similar phenotype, and forming phenotypically diverse cancer cells with more limited proliferative capabilities. [17]

The most classical experiment assessing the existence of cancer stem cells has been performed at the haematopoietic system. The haematopoietic system holds one of the most examined somatic stem cells in the body, the haematopoietic stem cells (HSCs), responsible for the generation and regeneration of blood cells. It had been observed that only a subset of cancer cells in leukemia and multiple myeloma are able to proliferate extensively. *In vitro* colony-forming assays with mouse myeloma cells displayed that only 1 in 10 000 to 1 in 100 cells are capable of forming colonies. *In vivo* transplants of leukaemic cells resulted in spleen colonies only in 1-4% of cells transplanted. Since the percentage of colony forming cells mirrored the proportion of HSCs among normal haematopoietic cells, the clonogenic leukaemic cells were designated as leukaemic stem cells. Obviously, there are two possible explanations to the scarce number of colonies formed, either all leukaemic cells could form colonies, but with a low probability or a small number of cells capable of acting as leukaemic stem cells existed. By separating leukaemic cells in distinct classes, John Dick and colleagues isolated a subgroup, distinguished as $CD34^{+}CD38^{-}$, exhibiting a high clonogenic capacity and exclusively capable of transferring human acute myeloid leukemia (AML) to NOD/SCID mice [18]. Employing cell surface markers in a similar methodology have extended the cancer stem cell principles to include breast cancer and glioblastoma [17].

The cellular origin of CSCs has not been established, although it seems likely that somatic stem cells, with dysregulated signaling pathways, are the raw material causing oncogenesis. There are two reasons why this might be true. First and foremost, multiple mutations have to

occur for a cell to initiate oncogenesis, implying that somatic stem cells, which might persist for long periods of time, can serve as life long reservoirs of mutations of possibly oncogenic nature. Therefore, somatic stem cells are more likely the source of CSCs in contrast to restricted progenitors and differentiated cells with commonly short lifespan. Second, since somatic stem cells already have the ability of self-renewal, a quality required by the CSCs, it seems convincing to propose CSCs to originate from somatic stem cells, although the possibility of progenitor/differentiated cells acquiring needed features of self-renewal also can occur (see Figure 3). [17]

The possible presence of cancer stem cells in solid tumors might be the explanation for metastatic features often observed in certain cancer forms. Furthermore, normal somatic stem cells tend to be more resistant to chemotherapeutics, possibly explained by ABC transporters capable of effluxing toxic compounds. If cancer stem cells are generated from dysregulated somatic stem cells this multidrug resistance might be inherited. Combining these proposed features one might be able to explain the recurrence of cancer, indicating therapies not aimed at cancer stem cells specifically to just reduce tumor size and not removing the major driving force of cancer (see Figure 4). [18]

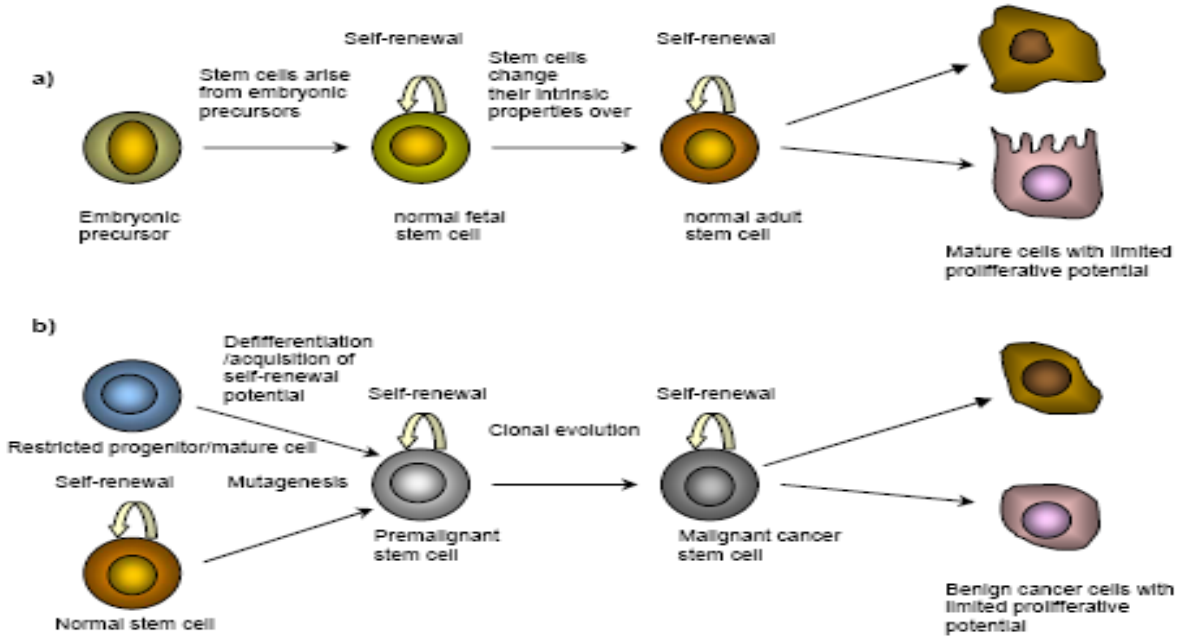

Figure 3. Parallels between a) development of normal tissues and b) generation of malignant tissues. Mutagenesis of a normal stem cell or possibly a restricted progenitor/mature cell acquiring self-renewal features initiates oncogenesis. Illustration adapted from [18].

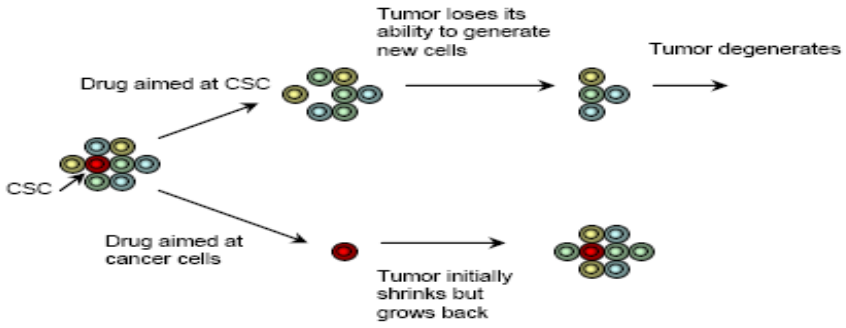

Figure 4. Chemotherapy may initially shrink tumor by killing cancer cells with limited proliferative capacity. Putative CSCs possibly more resistant to conventional therapies may remain viable and re-establish the tumor posterior of therapy. Drugs targeted at CSCs might not at first shrink tumor, but tumor loses its ability to generate new cells and eventually degenerates. Illustration adapted from [18].

3.7 Human lungs – epithelial stem cells and cancer stem cells

The human lungs are lined with epithelial cells and classically divided into four subdivisions: trachea, bronchi, bronchioles and alveoli. The complete lung system can be imagined as an inverted tree with the trachea being the tree trunk dividing into two branches, called bronchus, one to each lung. Inside the lung the bronchus branches into finer tubes called bronchioles ending as a cluster of air sacs called alveoli. [19]

The lung is a physically complex organ, which in contrast to other organs, such as blood, skin and gut, usually proliferate slowly. The epithelium of the lungs is constantly exposed to potentially toxic substances and pathogens in the close proximity of the organism. For this, epithelial lung cells must be quick and effective in response to cellular damage and local production of immune cytokines. Functionally and structurally appealing, models in the mouse have indicated lung stem cell populations, specific for each region, providing stem cell niches capable of local and rapid reaction when required [20]. That is, each subdivision of the lung holds its own stem cells: (i) basal and mucous secretory cells of the trachea; (ii) basal and mucous secretory cells of the bronchus; (iii) Clara cells of the bronchioles; (iv) type II pneumocyte cells of the alveoli [21]. Recently, a lung stem cell carrying Clara cell and alveolar-cell markers was discovered. When exposed to naphthalene treatment these double-positive cells started dividing, generating both Clara cells and alveolar type I and type II cells. Thus, they have a potential to act as progenitor to both Clara cells and alveolar cells and were therefore called bronchioalveolar stem cells. [22]

Lung cancers kill more people than any other cancer. Estimations regarding people in the West demonstrate lung cancers being more mortal than breast, cervical, colon and prostate cancer combined. Tragically, 90 % of all lung cancers are easily prevented being caused by cigarette smoking. Lung cancers are divided into several different neoplastic conditions defined by there unique phenotype and distinct regional location. Roughly, three major tumor types is utilized classifying lung cancer in a proximal-to-distal distribution, moving in a distal direction from the trachea these groups are squamous cell carcinoma (SCC), small cell lung carcinoma (SCLC) and adenocarcinoma/bronchoalveolar carcinomas. Data from mouse models indicate the presence of very particular regions of the airways, displaying tumorigenic features only when specific cellular mutations have occurred and the individual cell's local niche fosters cell growth. Observations also support Slaughter's 1953 carcinogenesis theory, in accordance with cancer stem cell theory, clonally expanded stem cells to be responsible for phenotypically similar lung cancer. Interestingly, recently identified stem cell niches, in the mouse, appear to overlap with sites originating adenocarcinoma/bronchoalveolar carcinomas, SCC and SCLC. [23]

SCCs in murine rarely develop in the distal region, but occur in the proximal airways down to the second or third bifurcation. Studying cells of SCC tumors, mutations commonly present in other lung cancer types is lacking, indicating the need for very specific mutations to occur in particular cell populations found among the proximal airway basal progenitors, to generate SCCs. Human SCLCs are mainly located to midlevel bronchioles and often express a high rate of metastatic dissemination. Pulmonary neuroendocrine cells (PNECs) have been proposed as origin of SCLC since they express neoroendocrine cell markers commonly seen in SCLCs. Moreover, evidences have displayed neuroepithelial body (NEB)-associated PNECs and SCLCs to utilize identical signaling pathways. Reactivity to SHH in NEBs is increased during lung development and repair-associated hyperplasia. Furthermore, overexpression of both SHH receptor and ligand is common in SCLC tumors, creating an

autonomous signaling, stimulating additional growth and bypassing the normal control mechanisms of NEB-associated proliferation. In murine models of central bronchiolar adenocarcinomas, the junction between the terminal bronchiole and the alveolus termed the “bronchoalveolar duct junction” (BADJ) has been reported as the regional starting point of these adenocarcinomas, and led to the hypothesis of Clara or alveolar type 2 (AT2) cells responsible for initiation of adenocarcinomas. When oncogenic protein K-ras is expressed either in vitro or in vivo, proliferation of exclusively bronchioalveloar stem cells are enhanced, indicating adenocarcinoma to originate from these stem cells. [23]

4 Strategy

This project have focused at screening an antibody library against primarily lung cancer cell lines for the expression of oncofetal antigens. It has also employed three other common cancers, namely colorectal cancer, pancreatic cancer and breast cancer, indicating if antigen is lung tissue specific. To confirm antigen of being cancerspecific and not just a commonly presented antigen myeloma cell line RPMI-8226 was used as a negative control in screening. The study was initiated by screening all antibodies on all cell lines twice in cell enzyme linked immunosorbent assay (CELISA). Candidates displaying negative signal on RPMI-8226 and positive signal on one or several cancer cell lines were studied further in western blotting and immunocytochemistry (ICC). Western blotting and ICC were carried out in two stages: (i) an initial step where antibodies were tested against RPMI-8226 and one or two cell lines interpreted as positive in CELISA; (ii) a follow up study screening specificity for all cell lines in this study as well as concentrated culture medium (western blotting). To further establish whether antigen is secreted, culture medium was test for blocking capacity in CELISA. Moreover, characterization of epitopes were performed applying periodate sensitivity measurements and random peptide library displayed by phages. Planned strategy is presented below in a flowchart (see Figure 5).

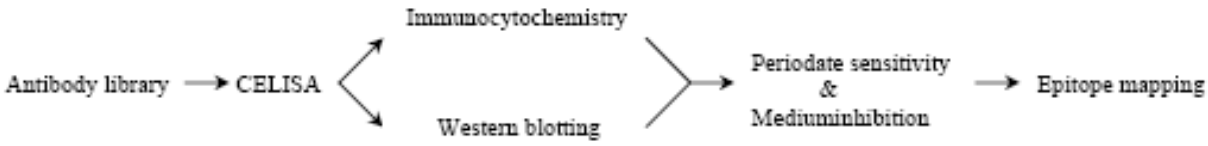

Figure 5. Flowchart of planned work

5 Materials and methods

5.1 Hybridoma library

Preceding this project, female Balb/c mice were immunized intraperitoneally with hES cells, early differentiated human hepatocyte cells (morphologically established), embryoid bodies and human feeder cells. Mice spleen cells were fused with myeloma cells (P3x63Ag8653II) and grown in 96 wells microplates on selective HAT-medium. Fusions resulted in 192 hybridomas (see Table 2). [Internal report, Fujirebio Diagnostics]

Table 2. Hybridoma antibody library used in screening for oncofetal antigens

Immunization cell	Hybridoma supernatants*
Human embryonic stem cells	HES 1-151
Human hepatocyte cells	HEP 1-4, 6, 9, 19, 22, 25-27, 29, 31-32, 34-35
Embryoid bodies	EB 2, 7-8, 10, 12, 14, 22-24, 26, 30, 32-33
Human feeder cells	HF 1-8, 10-12, 14

*Hybridoma supernatants contain 1-100 µg/ml immunoglobulin.

5.2 Cell culturing

Cells (see Table 3) stored in -140°C were thawed in lukewarm water and inoculated in inoculation medium {10% (v/v) fetal bovine serum (FBS) (Hyclone), 1% (v/v) dulbecco's modified eagle medium (DMEM) supplement (Gibco) in DMEM (Sigma)} (Except NCI-H345). Further culturing was performed at 37°C in 8.0% CO_2 (see Table 4 & 5). When reaching confluency cells growing adherently were collected applying trypsinization, diluted (1:4), sub-cultured in 96 wells microplates (Falcon) and allowed to reestablish for 40 h (in second experiment 30 000 cells were distributed per well). Cells on prepared microplates are shown in Table 6. Cells to be analyzed in western blotting were saved as cell pellets and cells for use in ICC were conserved in liqui PREP™ specimen preservative (LGM International) and stored at 4°C. To concentrate culture medium for western blotting, cells reaching 80% confluency were cultured for 48 h in medium lacking FBS. Culture medium were concentrated applying Amicon® Ultra centrifugal filter devices (Millipore) according to standard protocols.

Table 3. Cells cultured

Cell	ATCC	Organ	Disease
A427	HTB-53	Lung	Carcinoma
A549	CCL-185	Lung	Carcinoma
Calu-3	HTB-55	Lung	Adenocarcinoma
NCI-H69	HTB-119	Lung	Carcinoma/Small cell lung cancer
NCI-H345	HTB-180	Lung	Carcinoma/Small cell lung cancer
SK-MES-1	HTB-58	Lung	Squamous cell carcinoma
RPMI-8826	CCL-155	Peripheral blood	Plasmacytoma/Myeloma

Table 4. Culture medium

Culture medium	Medium contents
1	5% FBS, 1% DMEM supplement, DMEM
2	10% FBS, 1% DMEM supplement, DMEM
3	5% FBS, 1% DMEM supplement, 5 µg/ml insulin, IMDM*

* Iscove's modified dulbecco's medium.

Table 5. Growing conditions

Cell	Growth	Culture medium
A427	Adherent	1
A549	Adherent	1
Calu-3	Adherent	2
NCI-H69	Suspension/Multicell aggregates	1
NCI-H345	Suspension/Multicell aggregates/Some Adherent	3
SK-MES-1	Adherent	1
RPMI-8826	Suspension	1

Table 6. Cells on microplates prepared by project supervisor Karin Majnesjö

Cell	ATCC	Organ	Disease
Colo205	CCL-222	Colon	Colorectal adenocarcinoma
NCI-H128	HTB-120	Lung	Carcinoma/Small cell lung cancer
Panc1	CRL-1469	Pancreas	Epithelioid carcinoma
ZR75-1	CRL-1500	Mammary gland/breast	Ductal carcinoma

5.3 Fixation of cells in 96 wells microplates

5.3.1 Cells growing adherently

Culture medium was remove and cells gently washed twice with 300 µl phosphate buffered saline (PBS) pH 7.5. 50 µl of 4°C PBS was distributed and cells subsequently fixated by cross linking (see Appendix A for reaction) upon the addition of 50 µl ice-cold 0.5% (v/v) glutaraldehyde (Sigma) in PBS. Plates were incubated at room temperature (RT) for 13 min followed by two washes with PBS. 200 µl of 0.1% bovine serum albumin (BSA) (Sigma) in 100 mM glycine (Merck) in PBS were distributed and incubated at RT for 40 min to block any remaining aldehyde groups. Thereafter, plates were washed twice and 200 µl blocking solution {0.6% (w/v) trishydroxymethylaminomethane (TRIS) (Merck), 0.9% (w/v) NaCl (Merck), 0.05% (w/v) NaN_3 (Merck), 0.004 mM ethylenediaminetetraacetic acid (EDTA) (Merck), 0.045 mM $CaCl_2$ (Merck), 6% (w/v) D-sorbitol (Sigma) and 1.35% (v/v) stabilizer (Perkin Elmer)} was added. Subsequently, plates were blocked at 37°C for 45 min and stored at -20°C.

5.3.2 Cells growing in suspension

Cells growing in suspension were washed and resuspended in PBS. 50 µl of approximately 30 000 cells were distributed to each well in 96 wells microplates (Nunc) coated with poly-l-lysine (PLL) (Sigma). Thereafter, plates were centrifuged at 670 g for 5 min followed by an addition of 50 µl ice-cold 0.5% (v/v) glutaraldehyde (Sigma) in PBS. Following steps were performed in accordance with description above.

5.4 CELISA

Cells fixed in 96 wells microplates were thawed at 37°C for 45 min and washed three times with PBS. Then, 100 µl hybridoma supernatant diluted 1:2 in 2% (v/v) FBS (Hyclone) in PBS were added and incubated in humidified air at 4°C over night (ON). Hypoxanthine thymidine (HT) medium, used in hybridoma selection, were applied as negative control. The following day primary antibody was washed 4 times with washing buffer pH 7.75 {0.9% (w/v) NaCl (Merck), 0.1% (w/v) Germall II (Merck), 0.05% (w/v) tween20 (Merck) and 0.06% (w/v) TRIS (Merck)} with a subsequent addition of 100 µl secondary antibody solution {horseradish peroxidase (HRP) conjugated rabbit anti-mouse (Dako) diluted 1:1000 in 2%

(v/v) FBS (Hyclone), 1% (v/v) BSA (Roche) in PBS}. Plates were incubated in humidified air at RT for 2 h and thereafter washed four times. Then, 100 µl substrate solution {0.1% (w/v) o-phenylenediamine dihydrochloride (OPD) (Sigma) and 0.012% (v/v) H_2O_2 (Merck) in citrate buffer pH 5.0 [40 mM citric acid monohydrate (Merck) and 60 mM trisodium citrate dihydrate (Merck)]} were distributed and optical density (OD) measured at 450 nm applying a spectrophotometer (Molecular Devices) after 10 min.

5.5 Cell lysis

Cell lysates were produced applying lysis solution {1% triton X-100 (Sigma), 1 mM dithiothreitol (DTT) (Amersham biosiences), 0.2 mM phenylmethylsulphonyl fluoride (PMSF) (Sigma), 0.1 mM NaF (Merck) and one tablet of complete mini EDTA-free protease inhibitor (Roche) in milliQ water} to cell pellets. Pellets were solved in lysis solution and subsequently frozen in liquid nitrogen and thawed in an ultrasonic bath four times. Thereafter, samples were centrifuged at 400 g for 10 min and supernatants stored at -20°C.

5.6 The Bradford method

The Bradford method was performed in duplicates in 96 wells microplates applying dilution series. Bovine gamma globulin (BIO RAD Protein Assay Standard) was used as standard. 160 µl sample and 40 µl BIO RAD protein assay were distributed and incubated gently rocking at RT for 15 min. OD was measured at 620 nm employing a spectrophotometer (Molecular Devices).

5.7 Gel electrophoresis and western blotting

Gel electrophoresis and western blotting were performed in a NuPAGE® system applying standard protocols for gels and SDS running buffers in a XCell SureLock™ Mini-Cell (Invitrogen) (see Table 7). SimplyBlue™ SafeStain (Invitrogen) was utilized to ensure well separated protein equally distributed in all cell lysates. 10 µl samples {Cell lysate volume corresponding to 70 µg total protein content, 50 mM DTT and 2.5 µl NuPAGE® LDS sample buffer} were denatured at 70°C for 10 min prior to gel loading. SeeBlue® Plus2 Pre-Stained Standard (Invitrogen) and Magic Mark™ XP Western Standard (Invitrogen) were used as markers. Immun-Blot® PVDF membranes (BIO RAD) were prepared accord to standard protocol prior to blotting. Subsequent to blotting, membranes were washed brief twice in PBST {0.2% (w/v) tween20 (Merck) in PBS} and blocked at 4°C ON using blocking solution {5% (w/v) nonfat dry milk blotting grade blocker (BIO RAD) in PBST}. Membranes were incubated with pre-incubated hybridoma supernatant diluted in blocking solution gently rocking at RT for 1.5 h (see Table 7). Thereafter, membranes were washed three times gently rocking at RT for 15 min in approximately 200 ml PBST. Subsequently, membranes were incubated with pre-incubated secondary antibody {HRP conjugated rabbit anti-mouse (Dako) diluted 1:2000 in blocking solution} gently rocking at RT for 1.5 h followed by washing three times gently rocking at RT for 15 min in approximately 200 ml PBST. Bound antibodies were detected employing ECL Plus™ (Amersham Biosciences) and visualized on a Hyperfilm™ ECL™ (Amersham Biosciences) applying GBX developer and replenisher (Kodak) and GBX fixer and replenisher (Kodak). Film light and contrast were uniformly enhanced using Microsoft® Picture Manager.

Table 7. Applied dilution of hybridoma supernatant, and gel and buffer systems

Hybridoma supernatant	Dilution*	Gel	SDS Running buffer
HES6	1:20	12% Bis-Tris	MOPS
HES17	1:100	3-8% Tris-Acetate	Tris-Acetate
HES53	1:10	3-8% Tris-Acetate	Tris-Acetate
HES77	1:1000	3-8% Tris-Acetate	Tris-Acetate
HES99	1:1000	3-8% Tris-Acetate	Tris-Acetate
HES105	1:20	3-8% Tris-Acetate	Tris-Acetate
HEP4	1:1000	10% Bis-Tris	MOPS
HEP6	1:1000	10% Bis-Tris	MOPS
HEP34	1:1000	10% Bis-Tris	MOPS
HEP35	1:20	12% Bis-Tris	MOPS
EB2	1:500	10% Bis-Tris	MOPS
EB22	1:10	3-8% Tris-Acetate	Tris-Acetate
HF7	1:200	3-8% Tris-Acetate	Tris-Acetate

*1:20 dilution applied at first stage in western blotting.

5.8 ICC

Cells conserved in Liqui PREP™ specimen preservative (LGM International) were centrifuged at 1000 g for 10 min. Pellets were resolved in Liqui PREP™ cellular base solution (LGM International) and cells distributed on Polysine™ (Menzel) microscopic slides in 15 µl drops containing approximately 50 000 cells. Cells were allowed to adhere to slides at RT ON. Next day cells were rehydrated in 50% ethanol and washed with milliQ water and subsequently washed in PBS. Thereafter, 4% (w/v) paraformaldehyde (PFA) in PBS was utilized for 12 min to fixate cells by cross linking (see Appendix A for reaction), followed by three washes in PBS. Then, endogen peroxidases were inactivated upon addition of 5% H_2O_2. Subsequently, surface was blocked with irrelevant protein by incubating cells in 5% (v/v) heat inactivated (56°C for 30 min) FBS (Hyclone) in PBS at RT for 50 min. 100 µl hybridoma supernatant diluted 1:2 in 2% (v/v) heat inactivated FBS in PBS 2 were thereafter distributed and incubated in humidified air at RT for 1.5 h followed by three washes with 2% (v/v) heat inactivated FBS in PBS. Subsequently, secondary antibody, 1 µg/ml biotin conjugated goat anti-mouse immunoglobulin (Dako, biotinylated at Fujirebio Diagnostics), was added in 100 µl droplets, incubated in humidified air at RT for 1.5 h followed by three washes with 2% (v/v) heat inactivated FBS in PBS. Then, 100 µl of a tertiary ExtrAvidine perioxidase conjugate (Sigma) diluted 1:600 in PBS were apportioned and incubated in humidified air at RT for 1 h. After washing three times with 2% (v/v) heat inactivated FBS in PBS and a rinse in milliQ water, Sigma Fast™ 3,3-diaminobenzidine was dispensed in 60 µl droplets and incubated at RT for 20 min. Results were studied utilizing 40 times magnification light microscope (Carl Zeiss Axioskop) and photographed applying a Canon Powershot G6 kamera. Picture lightning and contrast were enhanced uniformly utilizing Microsoft® Picture Manager.

5.9 Periodate oxidation

Fixed cells in 96 wells microplates were equilibrated with 50 mM NaAc pH 4.5. 100 µl sodium metaperiodate in 50 mM NaAc pH 4.5, were added and incubated in the dark at RT for 1 h reducing original carbohydrate structures of antigens (see Appendix A for reaction). After 2 washes with PBST {0.05% (w/v) tween20 (Merck) in PBS}, 200 µl of 1% (w/v) glycine (Merck) in PBS were distributed and incubated at RT for 1 h to block any formed aldehyde groups. Wells were washed three times with PBST and subsequently used in CELISA as previously described.

5.10 CELISA mediuminhibition

Prior to loading of hybridoma supernatants in duplicates in CELISA, immunoglobulins were incubated with culture medium at 37°C for 2 h. Subsequent steps were performed as previously described in CELISA section.

5.11 Phage Display

96 wells microplates were incubated with 150 µl coating solution {100 µg/ml concentrated monoclonal antibodies in 0.2 M NaH_2PO_4 (Merck)} at RT ON. Coating solution was removed and 300 µl blocking solution, utilized in CELISA, was distributed and incubated at 37°C for 2 h. Blocking solution was cleared by washing with TBST {0.1% (v/v) tween20 (Merck) in tris buffered saline (TBS) pH 7.5)} 6 times. First panning reaction was performed by adding random peptide phage display library (Ph.D.-12 Phage Display Peptide Library, New England BioLabs) diluted in TBST according to standard protocol and incubating gently rocking at RT for 60 min. Plates were washed 10 times utilizing TBST to discard weakly binding phages. Phages strong positive for antibody were eluted by non-specific disruption of binding upon incubating in 100 µl acidic elution buffer {0.1% (w/v) BSA (Sigma) in 0.2 M glycine-HCl (Merck) pH 2.2} gently rocking at RT for 10 min. Subsequently, eluate was neutralized with 25 µl 1 M TRIS pH 8.3 and stored at 4°C. Phage content in eluates were determined by titering a small amount on LB agarose {1.5% agar (Merck) in LB medium [1% tryptone (Sigma) and 0.5% yeast extract (Sigma) pH 7.1]}/agarose top {0.7% agar (Merck) and 0.1% $MgCl_2$ in LB medium} petri dishes according to standard protocol. Eluate was amplified in a 20 ml ER2738 (New England BioLabs) early-log culture with vigorous shaking at 37°C for 4.5 h. Thereafter, cells were removed by centrifuging twice at 8200 g at 4°C for 10 min. Phage supernatant were precipitated with 1/6 volume of poly ethylene glycol (PEG) (Merck)/NaCl (Merck) at 4°C ON. Precipitates were purified and concentrated into amplified eluate according to standard protocol. The amplified eluates were titered in accordance with standard protocols on LB/agarose top petri dishes to clarify phage content in amplified eluates. The panning procedure with subsequent amplification was performed another 2 times with tween20 concentration raised to 0.5% (v/v) in all washing steps. After fourth round of panning, colonies were picked from titered LB/agarose top petri dishes. Clones were amplified and single-stranded phage DNA extracted according to standard protocol and sent for sequencing at Cybergene AB.

6 Results and discussion

The results and discussion section is separated into three segments. First, results from optimization and control experiments are presented. Second, a part featuring main results follows initiated by a results summary subsequently succeeded by a presentation and commentary of hybridoma supernatants results. Third, the work is discussed in a wider perspective motivating strategy, reporting observations made in the course of experiments and explaining possible sources of errors and their handling.

6.1 Optimization and control experiments

6.1.1 CELISA optimization

The average signal was lower for plates holding adherently growing cells, than for plates with cells fixed employing PLL. Combining this observation with performed dilution series displaying antigen as limiting factor, new plates were tested with more cells distributed in each well (see Appendix D). Also, reducing amount of washing repetitions (to three times) and decreasing detergent concentration (to 0.03% tween20) were tested to reduce the risk of acquiring false negative results. Unfortunately, this only resulted in higher background signal. Moreover, one cell line growing adherently (A549), was attached to plates employing PLL to compare results in the view of technique used (see Appendix D). When using PLL, signal is heighten in most cases in comparison with not applying PLL. However, if this is due to an enhancement of true or false signal is unclear.

6.1.2 Gel electrophoresis and the Bradford method

Coloring of all cell lysates applying a coomassie dye are shown in Figure 6. Clearly, all cell lysates contain well separated proteins in equal amounts. The Bradford method results enabled a maximum loading of RPMI-8226 at 70 µg total protein content (Data not shown).

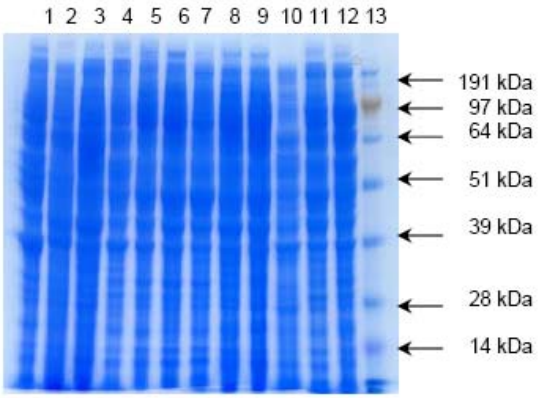

Figure 6. Cellysates of all tested cell lines. 1.A549 2.A427 3.Calu-3 4.SK-MES-1 5.NCI-H69 6.NCI-H345 7.NCI-H128 8.RPMI-8226 9.RPMI-8226 10.ZR75-1 11.Panc-1 12.Colo205 13.Marker

6.1.3 CELISA negative on RPMI-8226

To elucidate what value to interpreted as negative on RPMI-8226, E7 antibody (Fujirebio Diagnostics), most likely negative for RPMI-8226 (personal communication), were tested (see Table 8). Clearly, concentration of loaded antibody is vital. Cut-off value in selecting candidates for further studies were drawn at 0.25 (see RPMI-8226(3) in Appendix B).

Table 8. E7 antibody on RPMI-8226

	*RPMI-8226**		*RPMI-8226***	
50 *µg/ml*	0.568	0.541	0.339	0.342
25 *µg/ml*	0.411	0.361	0.215	0.223
10 *µg/ml*	0.175	0.149	0.112	0.149

*corresponds to RPMI-8226 and RPMI-8226(2) in Appendix B
**corresponds to RPMI-8226(3) in Appendix B

6.2 Results summary

Results outcome are presented in a flowchart in Figure 7. Results from CELISA are shown in Appendix B and C. ICC results are displayed in Appendix E. Furthermore, all results including hybridoma isotype are summarized in Table 9. 70 candidates were interpreted as negative for RPMI-8226 of these 24 (HES2, HES3, HES6, HES11, HES17, HES49, HES53, HES58, HES77, HES99, HES104, HES105, HES115, HES127, HES131, EB2, EB22, EB33, HEP4, HEP6, HEP9, HEP34, HEP35 and HF7) hybridoma supernatants being positive for one or several cell lines, were selected for further studies in western blotting and ICC. In western blotting EB33 and HES49 clearly visualized a specificity for RPMI-8226 and thus not further examined. Moreover, HES2, HES3, HES11, HES58, HES104, HES115, HES127, HES131 and HEP9 did not display any specific signal during stage 1 and thus not studied further in western blotting. In ICC HES2, HES3 and HES 131 were found specific for RPMI-8226 and thus not studied further. HES11, HES58, HES104, HES115, HEP9, and HEP35 did not display any positive signal during stage 1 and thus not studied further in ICC. 14 hybridoma supernatants (HES6, HES17, HES53, HES77, HES99, HES105, HES127, EB2, EB22, HEP4, HEP6, HEP34, HEP35 and HF7) were studied in periodate sensitivity measurements and mediuminhibition experiments. Finally, three purified and concentrated monoclonal antibodies (EB2, HEP34 and HF7) were tested applying random peptide phage display libraries.

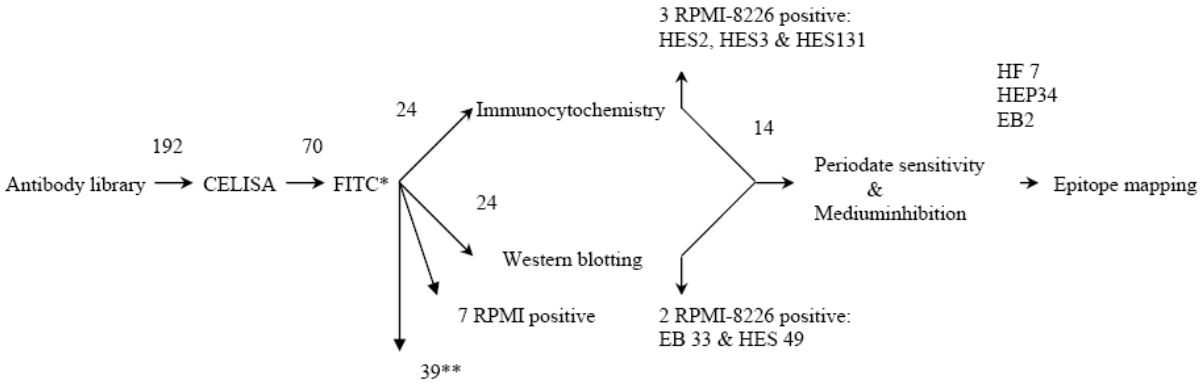

Figure 7. Flowchart of results outcome.
* Fluoresceinisotiocyanat (FITC) conjugated antibodies testing performed by Cellartis
** Not displaying signal enough in CELISA to be studied further

Table 9. Summary of results

	Isotype*	Mw (kDa)	Positive in western blotting/ ICC	Membranebound	Periodatsensitive	Secreted
HES6	G1	30	Western blotting: Calu-3, NCI-H345, NCI-H128, (A549, Colo205) ICC: Calu-3, NCI-H69, NCI-H345, Colo205	maybe	Yes	maybe
HES17	M	100-400	Western blotting: A549, Calu-3, SK-MES-1, Panc-1, Colo205 ICC: A549, Calu-3, SK-MES-1, (NCI-H345)	Yes	No	Yes
HES53	M	>400	Western blotting: Calu-3 ICC: Calu-3, SK-MES-1, NCI-H345, Colo205	Yes	No	Yes
HES77	M	100-400	Western blotting: Calu-3, (SK-MES-1) ICC: Calu-3	Yes	No	Yes
HES99	M (G2a)	100-400	Western blotting: Calu-3 ICC: Calu-3, (NCI-H128)	Yes	No	Yes
HES105	M	>400	Western blotting: A549, A427, Calu-3, Colo205 ICC: A549, Calu-3, SK-MES-1, NCI-H345, Colo205	Yes	Yes	Yes
HES127	M	?	Western blotting: - ICC: Calu-3, SK-MES-1, NCI-H345, Colo205	Yes	No	maybe
HEP4	G1(G3)	37-52	Western blotting: A549, A427, Calu-3, NCI-H69, NCI-H345, Panc-1, ZR75-1, Colo205, (NCI-H128, SK-MES-1) ICC: A549, A427, Calu-3, SK-MES-1, NCI-H69, NCI-H345, Panc-1, ZR75-1, Colo205, (NCI-H128)	Yes/No (granula in NCI-H69, NCI-H345, NCI-H128)	No	Yes
HEP6	G2b(M,G1)	37-52	Western blotting: A549, A427, Calu-3, SK-MES-1, NCI-H345, NCI-H69, NCI-H128, Panc-1, ZR75-1, Colo205 ICC: A549, A427, Calu-3, SK-MES-1, NCI-H345, NCI-H69, NCI-H128, Panc-1, ZR75-1, Colo205	Yes/No (granula in NCI-H69, NCI-H345, NCI-H128)	No	Yes
HEP34	G1	37-52	Western blotting: A549, A427, Calu-3, NCI-H345, NCI-H69, NCI-H128, Panc-1, ZR75-1, Colo205, (SK-MES-1) ICC: A549, A427, Calu-3, SK-MES-1, NCI-H345, NCI-H69, Panc-1, ZR75-1, Colo205	Yes/No (granula in NCI-H69, NCI-H345, NCI-H128)	No	Yes
HEP35	G2a	35	Western blotting: Panc-1 ICC: -	?	Yes	?
EB2	G1	40-48	Western blotting: A549, A427, Calu-3, NCI-H69, NCI-H128, Panc-1, ZR75-1, Colo205, (SK-MES-1, NCI-H345) ICC: A549, A427, Calu-3, , Panc-1, ZR75-1, Colo205, (NCI-H69, NCI-H345, NCI-H128)	Yes/No (granula in NCI-H69, NCI-H345, NCI-H128)	No	Yes
EB22	M(G1)	30, 70-100	Western blotting: A427, NCI-H69, NCI-H128 ICC: A427, NCI-H69, NCI-H128, (NCI-H345, ZR75-1)	Yes	Yes	Yes
HF7**	G1	160	Western blotting: Panc-1, SK-MES-1 ICC: SK-MES-1	Yes	No	Yes

* performed by Karin Majnesjö, project supervisor.
**tested in ICC with newly harvested SK-MES-1 cells.

6.3 Results of hybridoma supernatants

6.3.1 HEP4, HEP6, HEP34 & EB2

HEP4, HEP6, HEP34 and EB2 all showed signal resembles in CELISA, western blotting and ICC indicating a specificity for the same antigen or a variant of the same antigen. Band smears and multiple distinct bands was seen to divergent magnitude in all cell lines tested (except RPMI-8226) ranging from approximately 37 kDa to 52 kDa (see Figure 8 & Figure 9). EB2 are positive for a narrower antigen spectrum (40-48 kDa) than HEP4, HEP6 and HEP34 and thus denoting a divergent binding characteristics. HEP4, HEP6, and HEP34 also displayed a specificity at approximately 80 kDa found in Calu-3, Colo205 and Panc-1, even though at a much lesser intensity. Furthermore, in HEP6 two more bands were visible at >200 kDa in Calu-3 and at 20 kDa in A427. Antigen seems to be weakly expressed in easily seen distinct versions in small cell lung cancer cell lines. Alternative splicing and posttranslational modifications, such as glycosylations are possible explanations for this. Reducing immunoglobulin concentration might reveal similar bands in all other cell lines. All antibodies indicated to more or less extent the presence of antigen in concentrated NCI-H345 culture medium with HEP6 showing the strongest signal.

HEP4, HEP6, HEP34 and EB2 all gave similar expressions in ICC. Small cell lung cancers visualized a granular expression, whereas most other cell lines displayed an antigen of membrane bond character (see Figure 10). The existence of granulas also strengthens the observation of antigen being secreted, evidently seen in western blotting, interpreting granulas as vesicles transporting a secreted antigen. Mediuminhibition experiments only displayed HEP6 to be blocked by culture medium (see Figure 11), possibly explained by HEP6 having greater affinity for antigen than HEP4, HEP34, and EB2. Using concentrated culture medium may reveal antigen to be able to also block HEP4, HEP34, and EB2. HEP4, HEP6, HEP34, and EB2 all displayed no decreases in specificity upon periodate oxidation of fixed cells in CELISA. HEP34 and EB2 were selected for further studies using a random peptide library. Progress was determined by performing titration, revealing the ratio of output to input of phages for HEP34 to be increasing after every round of panning, whereas the ratio of EB2 phages were almost constant possibly denoting weak selection (see Figure 12). Unfortunately, sequencing individual phage clones selected for binding to HEP34 and EB2 did not result in any consensus sequence. In conclusion, since these 4 antibodies are positive for all cell lines tested to more or less extent, antigen may be a rather common structure presented by most cancer cells. Also, antigen were proven to be secreted and therefore applicable as a tumor marker.

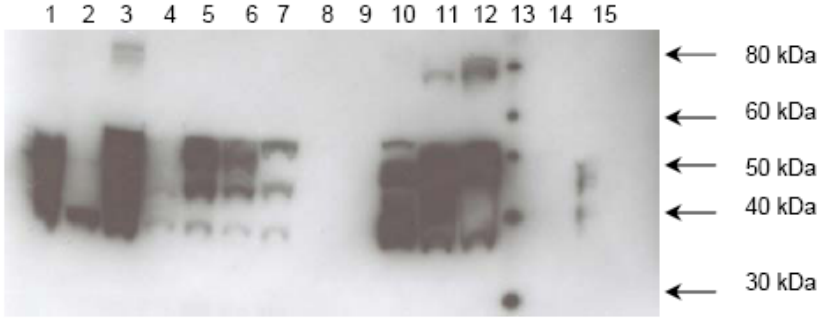

Figure 8. HEP34 western blotting. 1.A549 2.A427 3.Calu-3 4.SK-MES-1 5.NCI-H69 6.NCI-H345 7.NCI-H128 8.RPMI-8226 9.RPMI-8226 10.ZR75-1 11.Panc-1 12.Colo205 13.Marker 14.NCI-H69medium (concentrated 50:1) 15.NCI-H345medium (concentrated 50:1)

Figure 9. EB2 western blotting. 1.A549 2.A427 3.Calu-3 4.SK-MES-1 5.NCI-H69 6.NCI-H345 7.NCI-H128 8.RPMI-8226 9.RPMI-8226 10.ZR75-1 11.Panc-1 12.Colo205 13.Marker 14.NCI-H69medium (concentrated 50:1) 15.NCI-H345medium (concentrated 50:1)

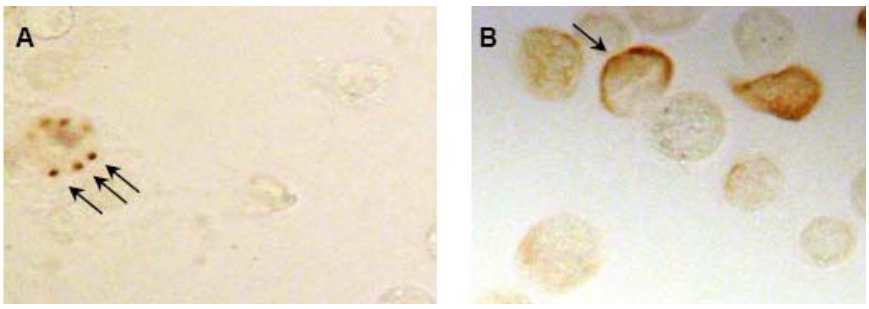

Figure 10. HEP6 displaying different pattern when bound to antigen present in (A) small cell lung cancer (NCI-H69) and (B) adenocarcinoma, (Calu-3). Arrows designate granular antigen in NCI-H69 and membrane bond antigen on Calu-3.

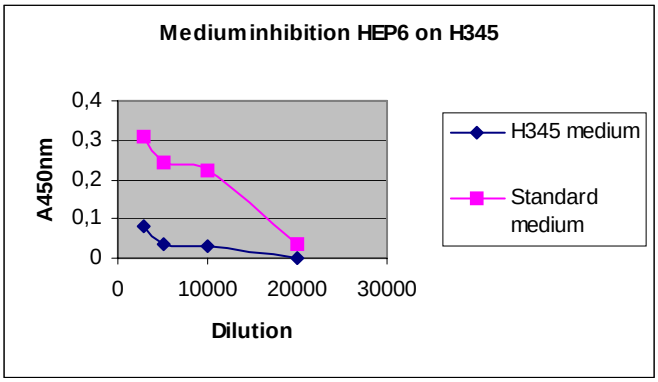

Figure 11. HEP6 antibody blocked by NCI-H345 culture medium.

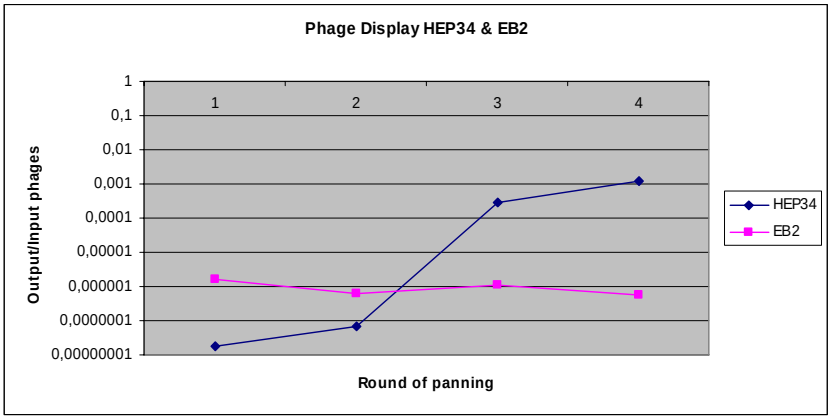

Figure 12. HEP34 exhibits an increasing amount of strong binding clones, whereas EB2 shows no increase in output/input of phages implying no selection of strong binding clones.

6.3.2 HES6

HES6 was positive for Calu-3, NCI-H128, NCI-H345 with western blotting at a molecular weight of 25-32 kDa (see Figure 13). Moreover, bands at 35-40 kDa were displayed in A427 and Colo205. No signal was seen on concentrated culture medium from A549 or NCI-H345. In ICC HES6 was positive on Calu-3, Colo205 and all small cell lung cancers. Signal, very easily seen in Colo205, indicated antigen to be concentrated at one side of the cell close to the membrane (see Figure 14). This pattern remains unexplained. HES6 indicated a decreased signal in blocking experiments in CELISA using culture medium from Calu-3 and H345, respectively, although effect was not of great magnitude. The epitope of HES6 was proven to be carbohydrate sensitive (see Table 10), converging with observed bands in western blotting indicating glycoprotein. In conclusion, in CELISA HES6 gave very high readings on multiple cancer cell lines, A549, Calu-3, NCI-H69 and NCI-H345 (also Colo205, H128, ZR75-1(data not shown), whereas being negative on RPMI-8226. Furthermore, HES6 was detected as positive for Calu-3, NCI-H345, NCI-H128 and Colo205 in both ICC and western blotting. Thus, these converging results are most likely true. If HES6 antigen can be proven to be secreted it is an interesting antigen for use as a tumor marker being highly expressed by cancer cell lines.

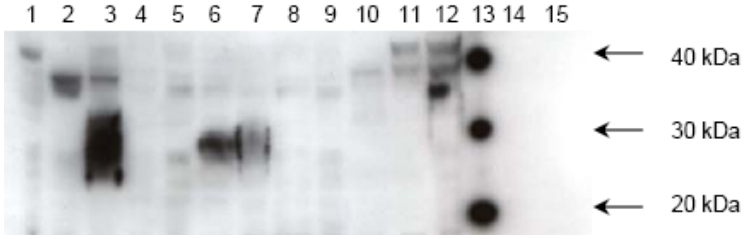

Figure 13. HES6 western blotting. 1.A549 2.A427 3.Calu-3 4.SK-MES-1 5.NCI-H69 6.NCI-H345 7.NCI-H128 8.RPMI-8226 9.RPMI-8226 10.ZR75-1 11.Panc-1 12.Colo205 13.Marker 14.A549medium (concentrated 100:1) 15.NCI-H345medium (concentrated 50:1)

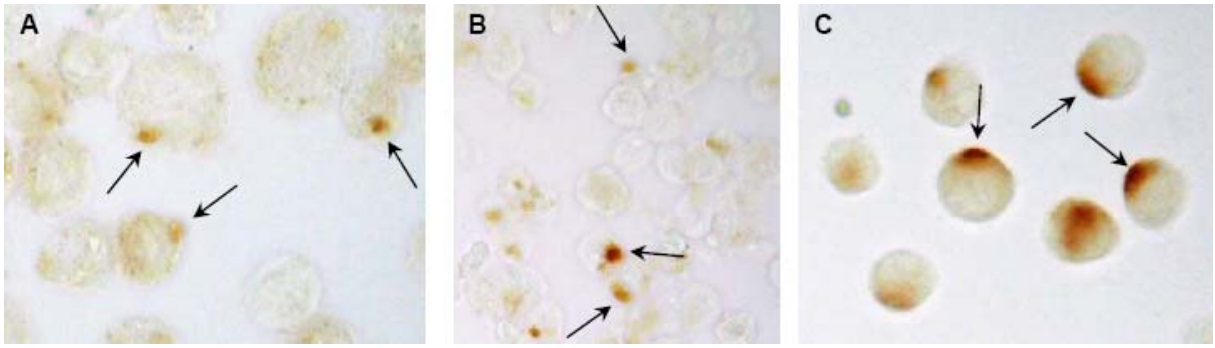

Figure 14. HES6 signal indicates asymmetrically distributed antigen in the close proximity of the membrane (A) Calu-3, (B) NCI-H69 and (C) Colo205

Table 10. HES6 in periodate oxidation of antigen presented on cells in CELISA

	0 mM	*0 mM*	*1 mM*	*1 mM*	*5 mM*	*5mM*	*10 mM*	*10 mM*	*100 mM*	*100 mM*
HES6*	0.086	0.091	0.100	0.107	0.010	0.010	0.005	0.009	0.002	0
HES6**	0.246	0.252	0.245	0.284	n/a	n/a	0.020	0.019	0.014	0.008

*antigen presented by Calu-3, HES6 dilution 1:3000

**antigen presented by NCI-H345, HES6 dilution 1:4000

Results interpretation: sensitivity for 1mM is a strong proof of carbohydrate dependent epitope, sensitivity for 1-10 mM indicates carbohydrate dependent epitope and insensitive for 100 mM is a strong proof of protein determinant [24].

6.3.3 HES105

In western blotting HES105 indicated specificity in a smear band >400 kDa for Calu-3 and Colo205, both adenomcarcinomas (see Figure 15). HES105 was also weakly positive for A549 and A427. The antigen of HES105 was evidently visualized present in concentrated A549 culture medium in western blotting. In ICC, HES105 showed specificity for A549, Calu-3, SK-MES-1, NCI-H345 and Colo205, thus also including small cell lung cancer NCI-H345 verifying observed results in CELISA (see Figure 16). Performing mediuminhibition in CELISA concentrated culture medium from NCI-H345 was used proving antigen to be secreted. Also, HES105 was proven to be sensitive to periodate oxidation indicating carbohydrate dependent epitope (see Table 11). In conclusion, HES105 could be positive for an antigen exclusively presented by adenocarcinomas as seen in western blotting. Therefore, retesting HES105 in ICC performing dilution series should be performed to separate specific from non-specific signal.

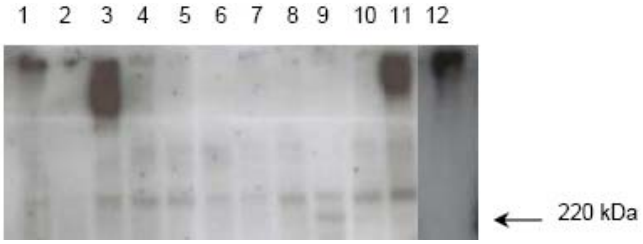

Figure 15. HES105 western blotting. 1.A549 2.A427 3.Calu-3 4.SK-MES-1 5.NCI-H69 6.NCI-H345 7.NCI-H128 8.RPMI-8226 9.ZR75-1 10.Panc-1 11.Colo205 12.A549medium (concentrated 100:1)

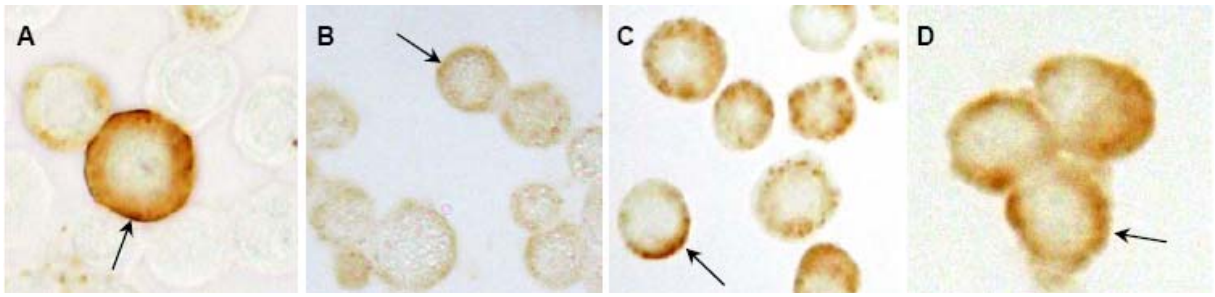

Figure 16. HES105 positive for a) A549 b) Calu-3 c) Colo205 d) NCI-H345. Arrows indicate membrane bound antigen.

Table 11. HES105 in periodate oxidation of antigen presented on cells in CELISA

	0 mM	*0 mM*	*1 mM*	*1 mM*	*10 mM*	*10 mM*	*100 mM*	*100 mM*
HES105*	0.190	0.191	0.279	0.274	0.004	0.001	0	0.002
HES105**	0.066	0.061	0.261	0.297	0	0	0.003	0.004

*antigen presented by NCI-H345, HES105 dilution 1:2
**antigen presented by A549, HES105 dilution 1:2

6.3.4 EB22

In CELISA EB22 gave positive results on A427, NCI-H69 and NCI-H128. In western blotting these results were confirmed by a 70-100 kDa smear band seen in NCI-H69 and a shorter band, 80-90 kDa, visible in A427 (see Figure 17). Also, signal was obtained at a molecular weight of 30 kDa in A427 and NCI-H128. The divergent molecular weights could be explained by the hybridoma supernatant being polyclonal. No signal was received on

concentrated culture medium from A549 and NCI-H69. In ICC EB22 displayed a positive signal on A427, NCI-H69, NCI-H128 and ZR75-1 with antigen being membrane bound. Staining of ZR75-1 was very intense and therefore this result need to be treated with caution. Mediuminhibition experiment applying concentrated NCI-H69 culture medium in CELISA clearly visualized EB22 to be secreted. EB22 was proven to be sensitive to carbohydrate degradation (see Table 12) by periodate oxidation. Thus indicating a carbohydrate dependent epitope. In conclusion, the main techniques used gave more or less the same result for EB22, indicating a shared antigen expression on A427, NCI-H69 and NCI-H128. Antigen is glycosylated, secreted and probably membrane bound. Interestingly, EB22 and EB33 are positive for the same cell lines and both showing low signal on RPMI-8226 in CELISA. Moreover, EB33 is an IgM immunoglobulin specific for a glycosylated, membranebound antigen of 35 kDa (data not shown), present on NCI-H128, NCI-H69, A427 and RPMI-8226. Therefore EB22 and EB33 might be positive for the same antigen and thus, EB22 may display a false negative signal on RPMI-8226.

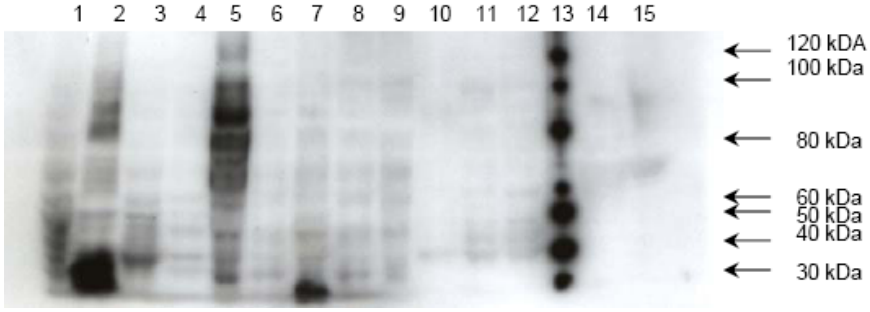

Figure 17. EB22 western blotting. 1.A549 2.A427 3.Calu-3 4.SK-MES-1 5.NCI-H69 6.NCI-H345 7.NCI-H128 8.RPMI-8226 9.RPMI-8226 10.ZR75-1 11.Panc-1 12.Colo205 13.Marker 14.A549medium (concentrated 100:1) 15.NCI-H69medium (concentrated 50:1)

Table 12. EB22 periodate oxidation of antigen presented on cells in CELISA

	0 mM	*0 mM*	*1 mM*	*1 mM*	*5 mM*	*5mM*	*10 mM*	*10 mM*	*100 mM*	*100 mM*
EB22*	0.175	0.171	0.168	0.191	n/a	n/a	0	0.002	0	0
EB22**	0.088	0.085	0.072	0.079	0	0.001	0.001	0.001	0.001	0.002

*antigen presented by NCI-H69, EB22 dilution 1:100
**antigen presented by A427, EB22 dilution 1:1000

6.3.5 HES17, HES77 & HES99

HES17, HES77 and HES99, all positive on Calu-3 in CELISA, displayed similar patterns in western blotting with a long smear band from approximately 100 kDa to 400 kDa on Calu-3 (see Figure 18). Thus, it is reasonable to propose that specificity for the same antigen exist. Whereas HES77 and HES99 only were specific for Calu-3, HES17 was also positive on A549, SK-MES-1 and Panc-1 at 100 kDa. SK-MES-1 also displayed a smear band in the range 200-400 kDa. Moreover, a weak but possibly specific signal was observed on RPMI-8226. Applying a much lower immunoglobulin concentration of HES17 only revealed positive signals on Calu-3 and SK-MES-1 (Data not shown). Concentrated culture medium from SK-MES-1 clearly indicated HES17 antigen of >400 kDa to be present in culture medium. HES17 in ICC largely confirmed observed results in western blotting and CELISA, giving positive signal on Calu-3, SK-MES-1 and A549 (see Figure 19). HES77 and HES99 displayed strong specificity for Calu-3 in ICC converging with observations from western blotting and CELISA. Utilizing concentrated Calu-3 culture medium in mediuminhibition experiments strongly suggested antigen to be secreted (see Figure 20). No carbohydrate dependence in epitopes of HES17, HES77 and HES99 could be proven, thus indicating

protein determinant. Antigen of HES17, HES77 and HES99 are highly interesting being largely secreted and mainly specific for one cancer cell line, Calu-3.

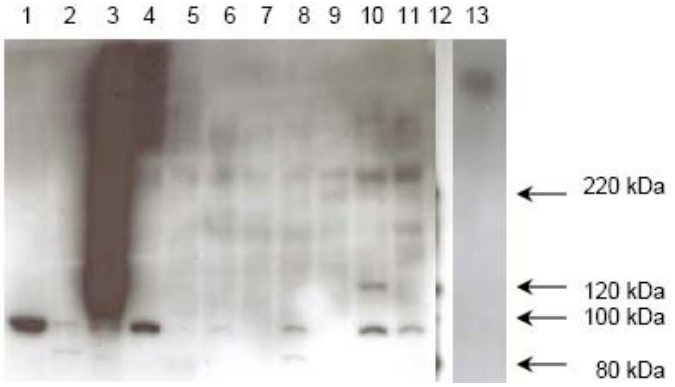

Figure 18. HES17 western blotting. 1.A549 2.A427 3.Calu-3 4.SK-MES-1 5.NCI-H69 6.NCI-H345 7.NCI-H128 8.RPMI-8226 9.ZR75-1 10.Panc-1 11.Colo205 12.Marker 13.SK-MES-1medium (concentrated 50:1)

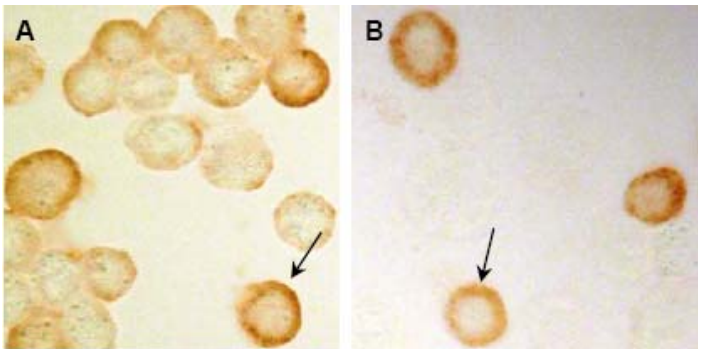

Figure 19. HES17 mainly positive for (A) Calu-3 and (B) SK-MES-1. Arrows indicate membrane bound antigen.

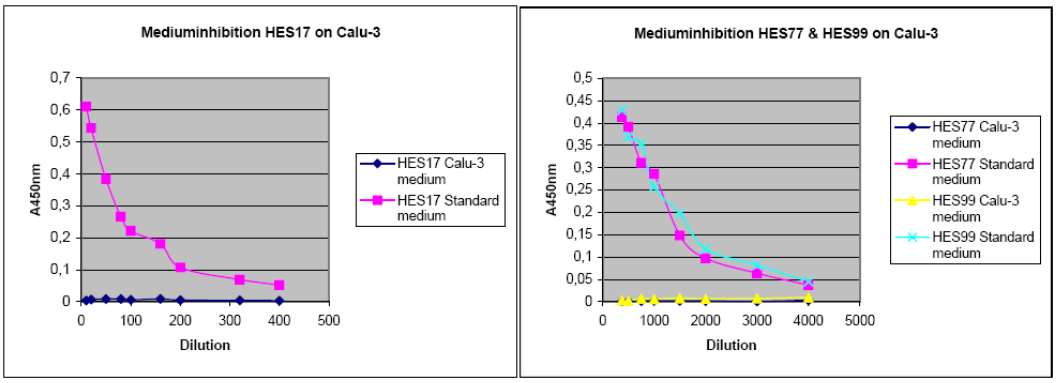

Figure 20. HES17, HES77 and HES99 antibodies inhibited completely by concentrated (10:1) Calu-3 culture medium.

6.3.6 HES53

HES53 displayed very low signal on RPMI-8226 in CELISA and a positive but weak signal on Calu-3 and NCI-H345. In western blotting HES53 displayed a specific, but weak smear band at >400 kDa on Calu-3 (see Figure 21). In ICC HES53 was positive for Calu-3, SK-MES-1 and NCI-H345 and Colo205 (see Figure 22) indicating membrane bound antigen. HES53 antigen was clearly proven to be present in concentrated NCI-H345 culture medium in

performing blockingexperiment in CELISA. No dependence of carbohydrate structures in HES53 epitope was observed and thus denoting epitope being composed of protein. ICC indicated antigen to be present in the membrane on Calu-3, NCI-H345, SK-MES-1 and Colo205, whereas western blotting only revealed one band (Calu-3), interpreted as specific, meaning results need to be verified in both western blotting applying a somewhat higher concentration and retesting HES53 in ICC using lower concentration.

Figure 21. HES53 western blotting. 1.A549 2.A427 3.Calu-3 4.SK-MES-1 5.NCI-H69 6.NCI-H345 7.NCI-H128 8.RPMI-8226 9.RPMI-8226 10.ZR75-1 11.Panc-1 12.Colo205 13.Marker

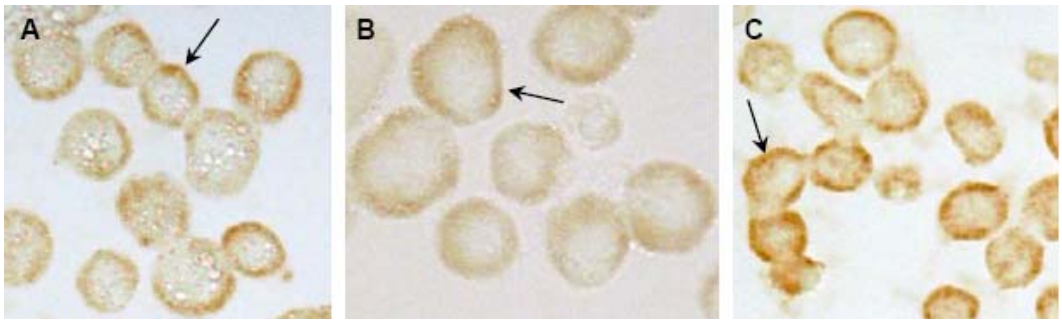

Figure 22. HES53 highly specific for (A) Calu-3 (B) SK-MES-1 and (C) NCI-H345. Arrows indicate membrane bound antigen.

6.3.7 HF7

Even though being raised against feeder cells, HF7 was interesting being equipped with specificity for an antigen exclusively presented by SK-MES-1 and Panc-1. This was proven in both CELISA and western blotting. Western blotting indicated an antigen molecular weight of approximately 160 kDa with a strong signal on SK-MES-1 and a somewhat weaker signal on Panc-1 (see Figure 23). By exposing film for 30 minutes western blotting revealed HF7 antigen to be present in SK-MES-1 culture medium. Furthermore, HF7 was tested on 5 additional cell lines, 3 pancreatic carcinomas: Paca2, ASPC-1 and BxPc3, and 2 ovarian squamous cell carcinomas: CaSki and HeLa. Interestingly, only ASPC-1 gave positive signal (Data not shown). HF7 gave no positive staining on cells stored in Liqui PREP™. However, on freshly harvested SK-MES-1 cells, HF7 antigen seems to be membrane bound (see Figure 24) converging with earlier observations (personal communication, Cellartis). Here, results need to be treated with caution since staining was very intense. Therefore retesting employing less immunoglobulin must be performed to clarify specific signal. Applying SK-MES-1 culture medium in western blotting and mediuminhibition experiments in CELISA (see Figure 25) prove HF7 to be secreted in low amounts. HF7 epitope are not sensitive to periodate oxidation and thus protein determinant is indicated. Furthermore, HF7 epitope was mapped successfully aligning three different clones resulting in a 5 aa consensus sequence (Data not shown) (see Figure 26). Performing a blastp search, applying confirmed molecular weight and information of antigen being membrane bound resulted in 1 possible protein (Data not shown)

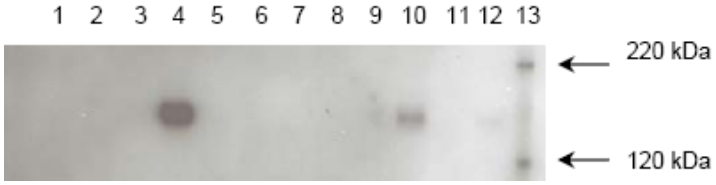

Figure 23. HF7 western blotting. 1.A549 2.A427 3.Calu-3 4.SK-MES-1 5.NCI-H69 6.NCI-H345 7.NCI-H128 8.RPMI-8226 9.ZR75-1 10.Panc-1 11.Colo205 12.SK-MES-1medium (concentrated 50:1) 13.Marker

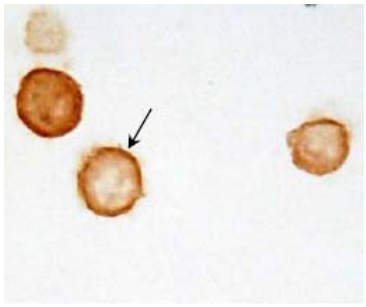

Figure 24. HF7 positive for freshly harvested SK-MES-1. Arrow indicate antigen to be membrane bound.

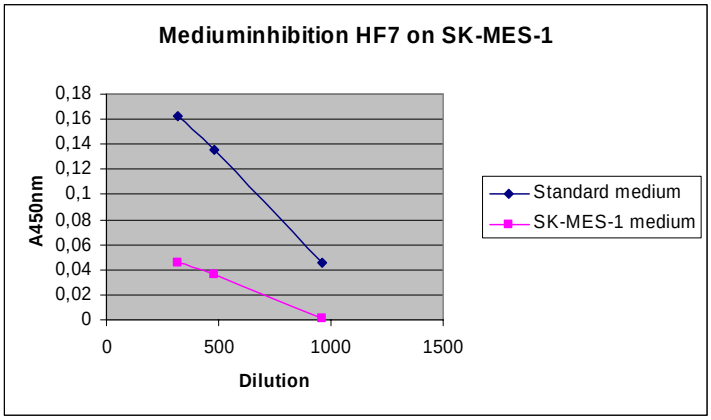

Figure 25. HF7 antibodies inhibited by concentrated (10:1) SK-MES-1 culture medium.

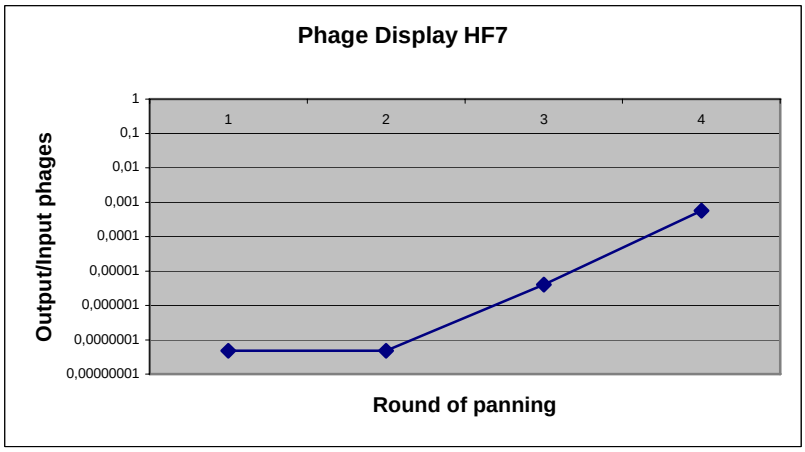

Figure 26. HF7 displays an expected development in phage display. At first panning most phages are washed away. Thereafter, output/input of phages is maintained constant since detergent concentration is raised between the first and second panning. At third and fourth panning output/input of phages are raised as more and more strong binding clones are selected as input to the next round of panning.

6.3.8 HEP35

HEP35 antigen, with a molecular weight of 35 kDa, was present in Panc-1 supporting observed data in CELISA (see Figure 27). In ICC no signal was received. HEP35 also displayed signal on A549 in CELISA, enabling mediuminhibitionexperiment and periodate sensitivity measurements in CELISA, although testing would ideally be performed on plates holding Panc-1. The epitope was found most likely composed of carbohydrate structures being sensitive to periodate oxidation (see Table 13). Interestingly, both HEP35 and HEP9 were mainly positive on Panc-1 and A549 possibly indicating similarities in these cell lines with the hepatocyte cells used in immunization. HEP35 is positive for mainly one cancer cell line, Panc-1. Therefore, testing other cancer cell lines with pancreatic origin should be interesting. Also, elucidating if antigen is secreted is vital if antigen is to be used as a tumor marker.

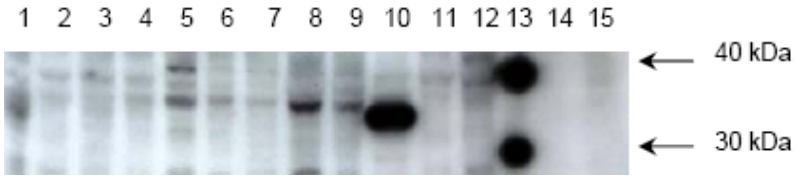

Figure 27. HEP35 western blotting. 1.A549 2.A427 3.Calu-3 4.SK-MES-1 5.NCI-H69 6.NCI-H345 7.NCI-H128 8.RPMI-8226 9.RPMI-8226 10.Panc-1 11.ZR75-1 12.Colo205 13.Marker 14.A549medium (concentrated 100:1) 15.NCI-H69 (concentrated 50:1)

Table 13. HEP35 in periodate oxidation of antigen presented on cells in CELISA

	0 mM	*0 mM*	*1 mM*	*1 mM*	*5 mM*	*5mM*	*10 mM*	*10 mM*	*100 mM*	*100 mM*
HEP35*	0.200	0.208	0.197	0.213	0.005	0.006	0.005	0.002	0.004	0

*antigen presented by A549, HEP35 dilution 1:1000

6.3.9 HES127

In ICC HES127 was positive for Calu-3, SK-MES-1, NCI-H345 and Colo205, whereas no signal was detected in western blotting. Thus, HES127 epitope is likely conformation dependent, with western blotting being performed in a reduced environment. Mediuminhibition in CELISA was measured employing concentrated NCI-H345 culture medium giving inconclusive results. HES127 epitope was not proven to be sensitivity to periodate oxidation and is therefore not dependent of carbohydrate structures.

6.4 Discussion

Screening an antibody library is a massive task. Applying a methodology gaining maximum information in minimum time should be prioritised. In this study an initial screening procedure was employed with a subsequent utilization of the results to select top candidates for further characterization. Clearly, this was a critical step in not rejecting any potent antibodies specific for oncofetal antigens. Therefore, a negative screening component had to be utilized in order to elucidate whether the antigen presented by lung cancer cells was of cancer specific nature or a commonly presented antigen also displayed on non-cancer cells. One apparent way would be to assign blood cells as negative screening material, but using blood cells clearly holds disadvantages such as handling and risk of contaminated blood. However, earlier studies screening cells for cancer specific antigens conducted during the 1980s, a time when hybridoma technologies producing monoclonal antibodies raised against

cancer cells were performed extensively, empirically validated the potential of myeloma RPMI-8226 as a negative control, even though being a cancer cell line [25].

When searching biomarkers, specific for cancer cells, to be used in diagnostic means the presence of cancer must be possible to detect. Primarily, the most obvious and best biomarker is a secreted antigen entering the blood circulation enabling detection in a serum sample. Secondarily, the biomarker could also be a membrane bound antigen possible to identify in a serum sample on circulating metastatic cells (CTCs) applying flow cytometry. Numerous studies have demonstrated monitoring CTCs count during cancer therapy can reflect the success of the treatment [26]. Thus, efforts have also been spent on elucidating whether possible oncofetal antigens are secreted and/or membrane bound.

In CELISA, performed twice testing reproducibility, two different techniques were employed, one method of sub-culturing adherently growing cells in microplates, and a second procedure immobilizing cells growing in suspension applying PLL. Clearly, one could argue only utilizing one technique would give more comparable results, but not using PLL for adherently growing cells can be motivate by allowing adherently growing cells to regain natural membrane surface following trypsinization. To ensure the presence of equal amounts of well separated proteins, protein staining with coomassie dye was performed. By applying the Bradford method equivalent amount of total protein content in samples could be loaded in western blotting enabling a partially quantitative interpretation of blots.

During this work the strength of practising several techniques has been highly appreciated. Results from western blotting, ICC and CELISA converged regarding a number of antibodies building a strong platform of convincing evidence. Also, RPMI-8226 were proven capable of giving positive signal in both western blotting and ICC, a critical feature for a negative screening tool to avoid accumulating a large number of false negatives.

Being a screen this study have focused at quantity, that is, prioritising the examination of multiple antibodies screened at several cell lines applying many techniques rather than concentrating on one or a few antibodies specificity at a couple of cell lines in one technique. Meaning, optimal conditions for all 192 antibodies have not been met, possibly biasing the final results. Mainly, the dependence of concentration in CELISA can not be disregarded since these results are applied in the critical step of selecting candidates for further studies. Here the risk of acquiring false positive results against RPMI-8826 due to non-specific binding of hybridoma supernatants expressing high amounts of immunoglobulin might disqualify interesting antibodies. Applying a lower concentration may reveal other antibodies, than those examined further here, to be negative for RPMI-8826 and specific on one or several cancer cells employed, that is, false positives decreased and true negatives increased on RPMI-8226. To eliminate this factor a time consuming cloning procedure has to be performed followed by a determination of immunoglobulin concentration. Determining immunoglobulin concentration in hybridoma supernatants linking antibody reactivity with antibody concentration is thus not possible. Cloning 192 hybridoma cultures before reaching any positive results are obviously not reasonable and therefore hybridoma supernatants were used. Even though, with more time a screen conducted utilizing more diluted samples in CELISA could have been fruitful.

Also, to further improve the opportunity of accomplishing excellent selection of candidates based on initial CELISA, a second screening tool could have been applied, analogous to RPMI-8226, representing common structures present on most cells. Introducing this extra

selection element more information would have been employed during the crucial step of choosing antibodies to study further. Furthermore, introducing a cell line originating from ectodermal tissue, such as neuroblastoma or malignt melanoma, might indicate possible primary germ layer specificity.

Since multiple antibodies were proven not to be working in western blotting and/or ICC, explanations for this need to be discussed here. Obviously, this observation can be due to a great number of factors and only some of them are explored here. At first, many antibodies selected for further studies were not displaying high signals in CELISA. Hybridoma supernatants indicating strong signals at many or most cell lines, including RPMI-8226, are most likely due to antigens being common structures presented by most human cells. High concentration could possibly also be an explanation as previously described. At the other end, selected hybridoma supernatants exhibiting low signals, in comparison to average signal, can be due to low amount of antigen and/or low concentration of antibodies. In practice, hybridomas producing low amounts of immunoglobulins are not applicable.

Furthermore, antigens can be sensitive to degradation, being depleted in cell extracts or not adequately preserved prior to ICC, exemplified by HF7 antigen proven to be present on fresh SK-MES-1 cells, whereas lacking on conserved SK-MES-1 cells. Moreover, trypsinization could possibly destroy sensitive membrane bound antigens for subsequent ICC studies. This problem were overcome in CELISA sub-culturing cells in wells, whereas cells used in ICC were not allowed to regain natural membrane surface. Also, antigen retrieval is sometimes needed to enhance antigen accessibility in ICC. Even though application of standard protocol could indicate intracellular signal, a permeabilisation process prior to fixation (not described) was performed to increase ability to reach intracellular antigens. Unfortunately, the procedure did not result in any new signals.

All results regarding IgM antibodies should be interpreted with larger skepticism than results received from IgG antibodies, because of the “sticky” nature of IgM antibodies. Also, the methodology of culturing cells for a short period in FBS free environment can be questioned. If cells cannot coupe with a low protein environment they might disintegrate leaking antigen into the culture medium rather than secreting the antigen. Moreover, dilution in periodate sensitivity measurement could perhaps also be questioned, although it seems intuitively correct to apply a concentration ensuring antibody of being a limiting factor to avoid a large non-specific signal.

One might argue screening antibodies against cancer cell lines in stead of cancer stem cells is not the right way to go. Applying cancer cell lines can be motivated with two arguments. First, cancer stem cells of the lungs have not been characterized today making the application of cancer stem cells impossible. Furthermore, assessing CSCs with cell surface markers the identification of antigens are already done. Second, the large majority of a tumors mass could be estimated to be made up of differentiated cancer cells producing measurable antigens possible to detect in cancer diagnosing. This should not be confused with therapy according to cancer stem cell theory aimed at eliminate the cause of malignancy, the CSCs.

7 Conclusions

A number of antigens, possibly of oncofetal nature, have been characterized. Multiple antigens have been proven to be secreted enabling their use as tumormarkers. Also, one characterized immunoglobulin indicates being specific for an antigen exclusively presented by adenocarcinomas. Furthermore, this project highlights the strength of applying multiple techniques to verify achieved results.

8 Future perspectives

For the future it would be interesting to screen the library at divergent hybridoma supernatant dilution to separate specific and non-specific signal in order to eliminate high signal being interpreted as specific signal, when in reality a high non-specific signal caused by high concentration could be biasing the results. Furthermore, as previously argued introducing yet another negative screening component would certainly provide valuable information regarding specificity for antigen present in most cells, although this might be to time consuming. Moreover, all results need to be verified utilizing an optimal concentration of antibody to confirm specificity in signal. Primarily ICC observations should be tested performing dilution series to elucidate specific signal.

Candidates viewed as interesting at this moment need to be more characterized. For this masspectrometry is a natural choice. Especially HF7 displaying high selective capacity and with epitope sequence known in combination with molecular weight and cellular location a complete identification is plausibly achievable.

In the end antibodies are meant to be employed in detecting oncofetal antigens in serum samples for diagnosing, monitoring and prognosing cancer. Therefore, testing candidates displaying interesting results in this early characterization on patient serum to perform a real testing of antibodies would be interesting. Furthermore, performing immunohistochemical studies on malignant tissues and normal tissues comparing reaction specificity displayed by antibodies should be highly rewarding.

9 Acknowledgments

At first I would like to acknowledge Olle Nilsson, Christian Fermér and Karin Majnesjö for letting me participate in this exciting project. I thank Christian Fermér and Karin Majnesjö for sharing their knowledge and for their enthusiastic, straightforward and helpful attitude. I thank Olle Nilsson for sharing his in-depth knowledge of tumor markers. Furthermore, I thank all the people at Fujirebio Diagnostics for making my stay a joyful time.

I would also like to thank my beloved family: my mother, Barbro Johansson, my father, Jan Johansson and my sister, Jenny Johansson, for their love and support.

10 References

1. Duffy, M. J. Clinical uses of tumor markers: a critical review. *Crit. Rev. Clin. Lab. Sci.* **38**, 225-262 (2001).

2. Farlex. The Free Dictionary: “oncofetal marker”. 2007. http://medicaldictionary.thefreedictionary.com/oncofetal+marker (Feb. 1, 2007).

3. Sarandakou, A., Protonotariou, E. & Rizos, D. Tumor markers in biological fluids associated with pregnancy. *Crit. Rev. Clin. Lab. Sci.* **44**, 151-178 (2007).

4. Duffy, M. J. Evidence for the clinical use of tumour markers. *Ann. Clin. Biochem.* **41**, 370-377 (2004).

5. Smith, A. A glossary for stem-cell biology. *Nature* **441**, 1060 (2006).

6. Vallier, L. & Pedersen, R. A. Human embryonic stem cells: an in vitro model to study mechanisms controlling pluripotency in early mammalian development. *Stem Cell Rev.* **1**, 119-130 (2005).

7. National Institutes of Health, U.S. Department of Health and Human Services. Appendix A: Early Development. 2006. http://stemcells.nih.gov/info/scireport/appendixa (May 22, 2007).

8. National Institutes of Health, U.S. Department of Health and Human Services. Stem Cell Basics: What are adult stem cells? 2006. http://stemcells.nih.gov/info/basics/basics4 (May 22, 2007).

9. Raff, M. Adult stem cell plasticity: fact or artifact? *Annu. Rev. Cell. Dev. Biol.* **19**, 1-22 (2003).

10. Thomson, J. A. *et al.* Embryonic stem cell lines derived from human blastocysts. *Science* **282**, 1145-1147 (1998).

11. Carpenter, M. K., Rosler, E. & Rao, M. S. Characterization and differentiation of human embryonic stem cells. *Cloning Stem Cells* **5**, 79-88 (2003).

12. Hoffman, L. M. & Carpenter M. K. Characterization and culture of human embryonic stem cells. *Nat. Biotechnol.* **23,** 699-708 (2005).

13. Andrews, P. W., Przyborski S. A. & Thomson J. A. Embryonal carcinoma cells as embryonic stem cells. *Cold spring Harbor Laboratory Press*, **Stem Cell Biology: Monograph 40** (2001).

14. Andrews, P. W. *et al.* Comparative analysis of cell surface antigens expressed by cell lines derived from human germ cell tumours. *Int. J. Cancer* **66**, 806-816 (1996).

15. Przyborski, S. A., Christie, V. B., Hayman, M. W., Stewart, R. & Horrocks G. M. Human embryonal carcinoma stem cells: models of embryonic development in humans. *Stem Cells Dev.* **13**, 400-408 (2004).

16. Burkert, J., Wright, N. A. & Alison, M. R. Stem cells and cancer: an intimate relationship. *J. Pathol.* **209**, 287-297 (2006).

17. Pardal, P., Clarke M. F. & Morrison S. J. Applying the principles of stem-cell biology to cancer. *Nat. Rev. Cancer* **3**, 895-902 (2003).

18. Reya, T., Morrison, S. J., Clarke, M. F. & Weissman, I. L. Stem cells, cancer and cancer stem cells. *Nature* **414,** 105-111 (2001).

19. Cambell, N. A., Reece, J.B. & Mitchell, L. G. Biology 5th edition. *Addison Wesley Longman,* **ISBN 0-8053-6573-7** (1999).

20. Rawlins, E. L. & Hogan, B. L. M. Epithelial stem cells of the lung: privileged few or opportunities for many? *Development* **133**, 2455-2465 (2006).

21. Otto, W. R. Lung epithelial stem cells. *J. Pathol.* **197**, 527-535 (2002).

22. Berns, A. Stem cells for lung cancer? *Cell* **121**, 811-813 (2005).

23. Giangreco, A., Groot, K. R. & Janes, S. M. Lung cancer and lung stem cells: strange bedfellows? *Am. J. Respir. Crit. Care. Med.* **175**, 547-553 (2007).

24. Johansson, C., Nilsson, O., Bäckström, D., Jansson, E. L. & Lindholm L. Novel epitopes on the CA50-carrying antigen: chemical and immunochemical studies. *Tumor Biol.* **12**, 159-170 (1991).

25. Lindholm, L. *et al.* Monoclonal antibodies against gastrointestinal tumor-associated antigens isolated as monosialogangliosides. *Int. Arch. Allergy Immunol.* **71**, 178-181 (1983).

26. Elshimali, Y. I. & Grody, W. W. The clinical significance of circulating tumor cells in the peripheral blood. *Diagn. Mol. Pathol.* **15**, 187-194 (2006).

27. Kiernan, J. A. Formaldehyde, formalin, paraformaldehyde and glutaraldehyde: What they are and what they do. *Microscopy Today* **1,** 8-12 (2000).

28. Solomons, T. W. G. Organic chemistry 6th edition. *John Wiley & Sons*, **ISBN 0-471-01342-0** (1996).

11 Appendix

11.1 Appendix A

11.1.1 Fixatives

Fixatives are employed to stabilize and preserve the fine structures in cells and tissues prior to observations in electron or light microscopy. The most commonly applied fixatives are aldehydes such as paraformaldehyde and glutaraldehyde capable of creating cross linking. Paraformaldehyde dissolves into small monomeric molecules, formaldehyde (HCHO), upon addition of heat gaining high potential of forming cross-linking (see Figure 28). Glutaraldehyde, a reasonably small molecule with one –CHO group at each side separated by a flexible 3 methylene bridge ($[-CH_2-]_3$) present in solution as polymers of different sizes, is utilized to create cross-linking between –CHO groups and $–NH_2$ groups according to Figure 29. [27]

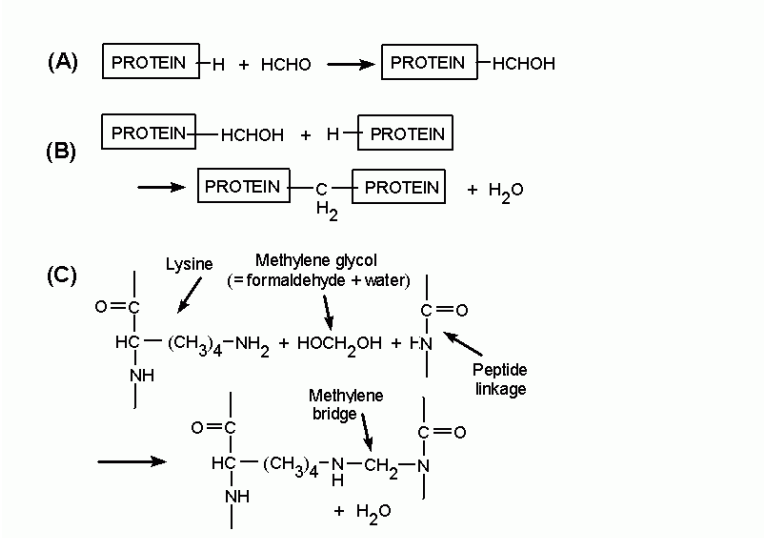

Figure 28. Fixation applying formaldehyde. **(A)** Addition of a formaldehyde molecule to a protein. **(B)** Reaction of bound formaldehyde with another protein molecule to form a methylene cross-link. **(C)** A more detailed depiction of the cross-linking of a lysine side-chain to a peptide nitrogen atom. Illustration used with permission from Microscopy Today.

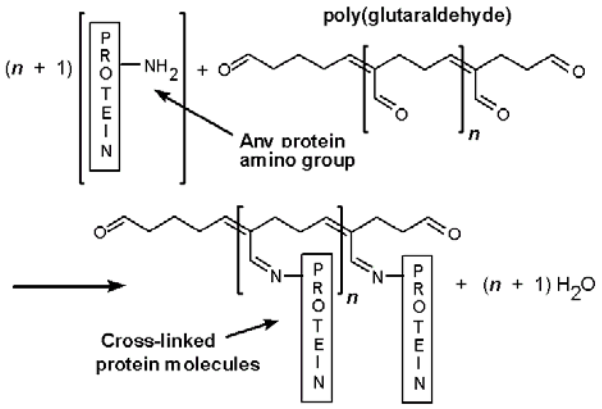

Figure 29. Reaction of poly(glutaraldehyde) with amino groups of proteins. Illustration used with permission from Microscopy Today.

11.1.2 Periodate oxidation

To establish possible carbohydrate dependence in antigen epitope binding displayed by an antibody, periodate oxidation can be utilized to cleave polyhydroxy compounds [26]. Treating compounds containing hydroxyl groups on adjacent atoms with aqueous periodic acid (HIO_4), carbon-carbon bonds are broken, producing carbonyl compounds (e.g. aldehydes) (see Figure 30) [28].

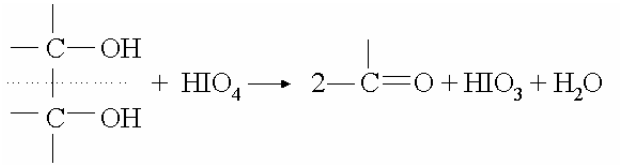

Figure 30. Periodate oxidation of carbohydrate.

11.2 Appendix B

11.2.1 CELISA complete results of A549, A427, Calu-3 and NCI-H345

	A549	A549 (2)	A427	A427 (2)	Calu-3*	NCI-H345	NCI-H345 (2)
HES1	0.009	0.003	0.015	0.009	0.007	0.135	0.028
HES2	0.064	0.051	0.016	0.006	0.008	0.484	0.217
HES3	0.221	0.230	0.129	0.037	0.129	0.426	0.184
HES4	-0.003	0.014	0.011	0.005	0.066	0.250	0.086
HES5	0.034	0.067	0.005	0.000	0.021	0.128	0.170
HES6	0.573	0.586	0.028	0.015	0.452	1.370	0.954
HES7	0.186	0.225	0.155	0.156	0.173	1.758	0.873
HES8	0.029	0.071	0.028	0.029	0.142	1.017	0.427
HES9	0.154	0.141	0.035	0.060	0.076	0.774	0.307
HES10	0.747	0.466	0.541	0.339	0.506	1.249	0.887
HES11	0.293	0.313	0.066	0.043	0.062	0.671	0.469
HES12	0.950	0.825	1.117	0.921	1.077	1.796	1.284
HES13	0.223	0.184	0.074	0.098	0.180	0.791	0.556
HES14	0.140	0.158	0.041	0.053	0.061	0.666	0.541
HES15	0.140	0.142	0.221	0.155	0.258	1.056	0.628
HES16	0.246	0.160	0.026	0.028	0.023	0.478	0.053
HES17	0.270	0.225	0.019	0.011	0.540	0.681	0.420
HES18	0.266	0.299	0.045	0.053	0.106	0.580	0.355
HES19	0.025	0.009	0.003	0.004	0.017	0.128	0.002
HES20	0.160	0.121	0.022	0.030	0.106	0.604	0.298
HES21	0.069	0.054	0.008	0.004	0.016	0.112	0.002
HES22	0.140	0.187	0.035	0.031	0.070	0.257	0.129
HES23	0.189	0.151	0.036	0.054	0.048	0.829	0.479
HES24	0.504	0.336	0.729	0.466	0.784	1.484	0.992
HES25	0.280	0.226	0.156	0.190	0.280	1.471	1.076
HES26	0.070	0.060	0.185	0.055	0.111	1.193	0.825
HES27	0.017	0.020	0.005	0.004	0.116	0.331	0.035
HES28	0.182	0.167	0.044	0.055	0.156	1.190	0.850
HES29	0.070	0.134	0.052	0.050	0.096	1.668	1.196
HES30	0.044	0.069	0.015	0.012	0.125	0.536	0.306
HES31	0.049	0.077	0.030	0.040	0.089	0.755	0.428
HES32	0.195	0.142	0.064	0.080	0.101	0.926	0.587
HES33	0.082	0.109	0.048	0.020	0.077	0.352	0.160
HES34	0.007	0.038	0.006	0.003	0.021	0.183	0.070
HES35	0.091	0.112	0.037	0.056	0.071	0.660	0.186
HES36	0.491	0.344	0.614	0.413	0.643	1.830	1.299
HES37	0.034	0.050	0.020	0.018	0.045	0.297	0.164
HES38	0.047	0.064	0.014	0.027	0.050	0.896	0.463
HES39	0.021	0.090	0.010	0.010	0.059	0.511	0.313
HES40	0.155	0.265	0.194	0.191	0.370	1.464	1.129
HES41	0.036	0.039	0.006	0.003	0.049	0.262	0.137
HES42	0.225	0.276	0.054	0.038	0.089	0.536	0.271
HES43	0.165	0.163	0.061	0.054	0.136	1.205	0.924
HES44	0.080	0.092	0.028	0.025	0.037	0.529	0.380
HES45	0.032	0.017	0.010	0.013	0.025	0.425	0.216
HES46	0.116	0.133	0.057	0.083	0.137	1.503	1.430
HES47	0.068	0.123	0.052	0.073	0.112	1.271	0.866
HES48	0.011	0.062	0.012	0.013	0.035	0.259	0.082
HES49	0.091	0.099	0.038	0.056	0.211	0.740	0.275
HES50	0.055	0.143	0.012	0.004	0.061	0.445	0.141
HES51	0.052	0.109	0.082	0.081	0.116	0.968	0.776
HES52	0.024	0.025	0.000	0.000	0.024	0.274	0.006

*Calu-3 only tested once

RPMI-8226 positive in FITC performed at Cellartis

	A549	A549 (2)	A427	A427 (2)	Calu-3*	NCI-H345	NCI-H345 (2)
HES53	0.133	0.114	0.002	-0.001	0.133	0.510	0.364
HES54	0.169	0.141	0.057	0.046	0.106	1.242	0.680
HES55	0.092	0.086	0.015	0.025	0.033	0.489	0.309
HES56	0.560	0.406	0.699	0.525	0.817	1.683	1.164
HES57	0.465	0.394	0.713	0.700	0.727	1.946	1.417
HES58	0.044	0.063	0.009	0.017	0.066	0.269	0.096
HES59	0.259	0.190	0.388	0.303	0.588	1.398	1.203
HES60	0.208	0.180	0.411	0.390	0.434	1.555	1.145
HES61	0.069	0.070	0.016	0.025	0.063	0.241	0.103
HES62	0.242	0.171	0.339	0.177	0.445	1.056	0.841
HES63	0.112	0.152	0.034	0.054	0.114	0.913	0.494
HES64	0.166	0.173	0.247	0.167	0.250	1.204	0.880
HES65	0.098	0.123	0.066	0.021	0.055	0.559	0.238
HES66	0.150	0.088	0.040	0.042	0.058	1.201	0.714
HES67	0.313	0.225	0.437	0.209	0.891	1.526	1.390
HES68	0.128	0.143	0.069	0.063	0.126	1.144	0.883
HES69	0.217	0.149	0.249	0.124	0.420	1.249	1.084
HES70	0.062	0.202	0.037	0.061	0.188	0.724	0.589
HES71	0.244	0.292	0.053	0.108	0.161	1.122	0.930
HES72	0.221	0.050	0.022	0.013	0.086	0.280	0.154
HES73	0.279	0.196	0.421	0.215	0.604	1.424	1.169
HES74	0.132	0.110	0.062	0.051	0.098	0.640	0.372
HES75	0.005	0.011	0.000	-0.003	0.010	0.029	-0.001
HES76	0.081	0.067	0.011	0.017	0.141	0.673	0.086
HES77	0.231	0.079	0.136	0.027	0.398	0.129	0.020
HES78	0.258	0.173	0.209	0.167	0.360	0.999	0.756
HES79	0.328	0.276	0.527	0.342	0.828	1.583	1.382
HES80	0.128	0.163	0.041	0.033	0.009	0.448	0.175
HES81	0.134	0.074	0.025	0.045	0.098	0.801	0.334
HES82	0.054	0.070	0.017	0.043	0.084	1.209	0.862
HES83	0.171	0.117	0.280	0.192	0.305	1.198	0.796
HES84	0.071	0.045	0.014	0.008	0.045	0.276	0.090
HES85	0.544	0.324	0.638	0.587	0.822	1.953	1.319
HES86	0.053	0.066	0.021	0.041	0.050	0.992	0.812
HES87	0.203	0.153	0.162	0.116	0.101	1.422	0.868
HES88	0.083	0.045	0.014	0.013	0.010	0.189	0.135
HES89	0.033	0.172	0.015	0.024	0.011	0.471	0.377
HES90	0.044	0.110	0.026	0.010	0.006	0.624	0.129
HES91	0.053	0.268	0.087	0.016	0.123	0.682	0.463
HES92	0.029	0.100	0.008	0.023	0.007	0.147	0.044
HES93	0.074	0.142	0.018	0.007	0.023	0.482	0.182
HES94	0.040	0.228	0.053	0.066	0.027	0.683	0.253
HES95	0.084	0.165	0.022	0.026	0.024	0.577	0.120
HES96	-0.001	0.132	0.019	0.019	0.027	0.365	0.340
HES97	0.064	0.194	0.016	0.019	0.024	0.300	0.192
HES98	0.594	0.719	0.104	0.151	0.364	0.424	0.223
HES99	0.014	0.072	0.008	0.053	0.309	0.055	0.006
HES100	0.040	0.111	0.013	0.011	0.009	0.121	0.020
HES101	0.134	0.390	0.175	0.097	0.074	0.700	0.500
HES102	0.083	0.203	0.077	0.059	0.173	0.833	0.808
HES103	0.049	0.148	0.030	0.040	0.128	0.649	0.150
HES104	0.048	0.175	0.027	0.036	0.025	0.193	0.348
HES105	0.181	0.293	0.005	0.006	0.156	0.598	0.362
HES106	0.101	0.191	0.099	0.127	0.208	1.082	0.583
HES107	0.038	0.107	0.030	0.061	0.042	0.589	0.329
HES108	0.092	0.089	0.002	0.005	0.013	0.143	0.030
HES109	0.021	0.046	-0.003	0.007	0.006	0.089	-0.001

*Calu-3 only tested once

RPMI-8226 positive in FITC performed at Cellartis

	A549	A549 (2)	A427	A427 (2)	Calu-3*	NCI-H345	NCI-H345 (2)
HES110	0.085	0.166	0.049	0.054	0.072	0.534	0.227
HES111	0.658	0.585	0.788	0.493	0.421	2.131	1.434
HES112	0.145	0.346	0.162	0.075	0.068	0.667	0.385
HES113	0.127	0.287	0.213	0.068	0.099	0.922	0.429
HES114	0.086	0.349	0.101	0.109	0.088	0.648	0.375
HES115	0.189	0.172	0.073	0.042	0.089	0.646	0.229
HES116	0.042	0.138	0.020	0.038	0.037	0.250	0.102
HES117	0.076	0.487	0.110	0.109	0.101	0.657	0.476
HES118	0.016	0.146	0.006	0.018	0.030	0.205	0.299
HES119	0.219	0.271	0.308	0.274	0.437	1.552	0.952
HES120	0.019	0.064	0.000	0.004	0.011	0.027	0.001
HES121	0.211	0.324	0.325	0.080	0.238	2.013	1.144
HES122	0.053	0.068	0.014	0.009	0.030	0.144	0.018
HES123	0.158	0.240	0.172	0.123	0.336	0.845	0.694
HES124	0.191	0.265	0.208	0.139	0.211	1.160	0.987
HES125	0.206	0.368	0.367	0.052	0.233	2.155	1.471
HES126	0.042	0.095	0.014	0.012	0.065	0.595	0.134
HES127	0.133	0.217	0.005	0.007	0.093	0.329	0.337
HES128	0.034	0.104	0.005	0.000	0.023	0.185	0.111
HES129	0.041	0.136	0.008	0.026	0.035	0.103	0.054
HES130	0.017	0.113	0.006	0.008	0.027	0.152	0.078
HES131	0.055	0.204	0.029	0.038	0.029	0.355	0.326
HES132	0.469	0.756	0.769	0.680	0.654	1.660	1.097
HES133	0.088	0.180	0.093	0.112	0.059	1.461	0.836
HES134	0.121	0.198	0.168	0.092	0.077	1.202	0.818
HES135	0.062	0.159	0.057	0.015	0.036	0.607	0.106
HES136	0.354	0.379	0.506	0.379	0.322	1.630	1.066
HES137	0.430	0.497	0.705	0.515	0.486	1.972	1.383
HES138	0.089	0.177	0.106	0.066	0.107	0.670	0.425
HES139	0.277	0.416	0.225	0.150	0.141	1.133	0.912
HES140	0.214	0.336	0.452	0.261	0.263	1.527	0.787
HES141	0.129	0.314	0.204	0.151	0.249	1.659	0.962
HES142	0.604	0.761	0.770	0.661	0.724	1.982	1.196
HES143	0.318	0.394	0.471	0.341	0.334	1.284	0.903
HES144	0.077	0.317	0.050	0.063	0.051	1.414	1.325
HES145	0.747	0.810	0.207	0.180	0.425	0.827	0.542
HES146	0.170	0.456	0.225	0.161	0.184	1.802	1.249
HES147	0.944	1.219	0.445	0.286	0.524	1.622	1.176
HES148	0.251	0.250	0.314	0.191	0.390	1.243	0.901
HES149	0.194	0.290	0.319	0.223	0.208	1.525	1.290
HES150	0.019	0.122	0.031	0.026	0.037	0.259	0.189
HES151	0.117	0.278	0.161	0.167	0.137	1.203	0.882
HEP1	0.014	0.189	0.059	0.097	0.059	0.676	0.455
HEP2	0.130	0.399	0.115	0.258	0.150	0.728	0.449
HEP3	0.039	0.113	0.027	0.024	0.041	0.318	0.182
HEP4	0.058	0.220	0.036	0.021	0.135	0.690	0.485
HEP6	0.151	0.329	0.134	0.084	0.366	0.944	0.779
HEP9	0.233	0.394	0.044	0.019	0.077	0.202	0.073
HEP19	0.149	0.273	0.116	0.085	0.097	1.284	1.251
HEP22	0.187	0.377	0.348	0.306	0.284	1.665	1.108
HEP25	0.128	0.476	0.139	0.144	0.137	1.052	0.734
HEP26	0.053	0.287	0.010	0.006	0.038	0.266	0.024
HEP27	0.032	0.221	0.056	0.029	0.089	0.835	0.642
HEP29	0.027	0.216	0.029	0.039	0.111	0.146	0.072
HEP31	0.047	0.152	0.021	0.066	0.037	0.586	0.293
HEP32	0.012	0.058	0.005	0.002	0.019	0.073	0.023
HEP34	0.059	0.185	0.022	0.027	0.109	0.526	0.373

*Calu-3 only tested once

RPMI-8226 positive in FITC performed at Cellartis

	A549	A549 (2)	A427	A427 (2)	Calu-3*	NCI-H345	NCI-H345 (2)
HEP35	0.186	0.333	0.042	0.039	0.059	0.254	0.093
EB2	0.090	0.255	0.050	0.068	0.198	0.357	0.177
EB7	0.576	0.407	0.591	0.639	0.536	1.940	1.359
EB8	0.090	0.270	0.073	0.167	0.123	1.280	1.336
EB10	0.731	0.671	0.928	0.601	0.656	2.191	2.014
EB12	0.219	0.371	0.060	0.046	0.093	0.340	0.126
EB14	0.177	0.387	0.240	0.163	0.250	1.446	1.072
EB22	0.033	0.065	0.195	0.151	0.063	0.379	0.294
EB23	0.132	0.350	0.109	0.182	0.128	1.413	0.987
EB24	0.126	0.243	0.094	0.171	0.120	1.120	0.977
EB26	0.275	0.310	0.098	0.066	0.187	1.592	1.217
EB30	0.293	0.332	0.120	0.110	0.305	1.671	0.963
EB32	0.333	0.334	0.168	0.159	0.159	1.736	1.121
EB33	0.104	0.099	0.206	0.130	0.055	0.225	0.245
HF1	0.368	0.303	0.051	0.040	0.131	0.154	0.035
HF2	0.047	0.061	0.006	0.005	0.016	0.104	0.176
HF3	0.247	0.230	0.099	0.087	0.109	1.123	0.785
HF4	0.155	0.106	0.042	0.048	0.023	0.555	0.075
HF5	0.368	0.424	0.405	0.404	0.609	1.011	0.595
HF6	0.063	0.111	0.007	0.023	0.024	0.082	0.005
HF7	0.138	0.133	0.004	0.004	0.026	0.073	0.014
HF8	0.349	0.398	0.249	0.229	0.264	1.926	1.346
HF10	0.487	0.597	0.462	0.473	0.439	1.579	1.063
HF11	0.262	0.248	0.089	0.114	0.226	0.946	0.489
HF12	0.166	0.276	0.030	0.036	0.029	0.133	0.287
HF14	0.273	0.310	0.072	0.050	0.112	0.865	0.421

*Calu-3 only tested once

RPMI-8226 positive in FITC performed at Cellartis

11.2.2 CELISA complete results of NCI-H69, SK-MES-1 and RPMI-8226

	NCI-H69	NCI-H69 (2)	SK-MES-1	SK-MES-1 (2)	RPMI-8226	RPMI-8226 (2)	RPMI-8226 (3)*
HES1	0.179	0.211	0.009	0.004	0.213	0.275	0.060
HES2	0.273	0.641	0.049	0.067	0.085	0.194	0.070
HES3	0.442	0.517	0.064	0.100	0.170	0.316	0.123
HES4	0.149	0.258	0.005	0.011	0.125	0.171	0.027
HES5	0.134	0.200	0.007	0.003	0.017	0.014	0.018
HES6	0.987	1.307	0.023	0.014	0.087	0.091	0.038
HES7	1.305	1.850	0.181	0.317	1.174	1.927	1.177
HES8	0.501	0.750	0.045	0.032	0.859	1.460	0.373
HES9	0.417	0.667	0.043	0.076	0.699	1.056	0.448
HES10	1.383	1.696	0.416	0.662	0.778	1.004	1.184
HES11	0.486	0.868	0.033	0.057	0.487	0.997	0.181
HES12	1.242	1.587	1.023	1.314	1.421	2.195	1.250
HES13	0.666	0.741	0.339	0.190	0.613	1.066	0.480
HES14	0.526	0.602	0.088	0.098	0.595	0.923	0.267
HES15	0.836	1.049	0.173	0.199	0.831	1.000	0.583
HES16	0.066	0.410	0.011	0.013	0.317	0.340	0.170
HES17	0.126	0.183	0.135	0.186	0.059	0.151	0.010
HES18	0.505	0.672	0.066	0.093	0.529	0.973	0.297
HES19	0.082	0.194	0.005	0.002	0.008	0.004	0.008
HES20	0.515	0.769	0.050	0.059	0.526	0.805	0.336
HES21	0.091	0.133	0.005	0.003	0.012	0.014	0.012
HES22	0.359	0.474	0.060	0.055	0.199	0.266	0.157
HES23	0.433	0.506	0.071	0.046	0.869	1.429	0.342
HES24	1.008	1.291	0.632	0.945	1.204	1.816	1.064
HES25	1.020	1.255	0.250	0.296	1.265	2.004	1.092
HES26	0.750	1.284	0.074	0.108	0.850	1.677	0.742
HES27	0.105	0.356	0.005	0.011	0.041	0.078	0.012
HES28	0.732	1.029	0.091	0.134	0.814	1.377	0.650
HES29	0.950	1.117	0.046	0.111	1.307	2.276	1.027
HES30	0.258	0.504	0.016	0.035	0.439	1.096	0.122
HES31	0.598	0.675	0.072	0.093	0.353	0.593	0.381
HES32	0.386	0.843	0.088	0.105	0.658	1.192	0.492
HES33	0.418	0.618	0.020	0.043	0.207	0.325	0.227
HES34	0.207	0.264	0.011	0.010	0.127	0.268	0.083
HES35	0.456	0.713	0.092	0.082	0.287	0.452	0.227
HES36	1.544	1.849	0.471	0.701	1.397	2.204	1.426
HES37	0.248	0.250	0.033	0.029	0.277	0.471	0.078
HES38	0.280	0.487	0.054	0.062	0.796	1.463	0.211
HES39	0.447	0.474	0.009	0.032	0.435	0.752	0.245
HES40	1.065	1.403	0.254	0.285	1.372	2.301	0.890
HES41	0.202	0.280	0.011	0.019	0.167	0.455	0.085
HES42	0.428	0.524	0.124	0.117	0.593	0.799	0.410
HES43	0.666	0.971	0.137	0.130	1.130	1.913	0.749
HES44	0.460	0.575	0.034	0.042	0.475	0.706	0.262
HES45	0.380	0.574	0.029	0.029	0.388	0.553	0.195
HES46	0.960	1.159	0.169	0.145	1.362	2.343	1.069
HES47	0.552	0.628	0.100	0.110	1.131	1.661	0.748
HES48	0.198	0.222	0.014	0.030	0.169	0.352	0.046
HES49	0.585	0.880	0.197	0.263	0.337	0.468	0.232
HES50	0.404	0.441	0.064	0.060	0.583	0.862	0.210
HES51	0.653	0.933	0.118	0.150	0.892	1.406	0.743
HES52	0.118	0.138	0.008	0.004	0.500	0.861	0.033
HES53	0.102	0.204	0.007	0.012	0.011	0.142	0.009
HES54	0.616	0.762	0.119	0.141	0.976	1.497	0.656

*RPMI-8226(3) and RPMI-8226(1,2) fixed at different occasion

RPMI-8226 positive in FITC performed at Cellartis

	NCI-H69	NCI-H69 (2)	SK-MES-1	SK-MES-1 (2)	RPMI-8226	RPMI-8226 (2)	RPMI-8226 (3)*
HES55	0.426	0.611	0.041	0.053	0.467	0.734	0.264
HES56	1.305	1.791	0.560	0.810	1.678	1.994	1.506
HES57	1.736	2.059	0.610	0.829	1.663	2.212	1.871
HES58	0.228	0.222	0.033	0.028	0.326	0.383	0.079
HES59	1.733	1.902	0.318	0.409	1.078	1.545	1.588
HES60	1.357	1.688	0.406	0.615	1.194	2.107	1.518
HES61	0.495	0.588	0.039	0.038	0.429	0.585	0.338
HES62	1.405	1.645	0.240	0.264	0.681	1.024	1.282
HES63	0.580	0.850	0.125	0.104	0.630	0.972	0.545
HES64	1.386	1.622	0.120	0.161	0.778	1.300	1.233
HES65	0.384	0.573	0.062	0.061	0.383	0.471	0.313
HES66	0.705	0.718	0.078	0.086	0.878	1.299	0.831
HES67	1.679	1.962	0.434	0.348	1.306	1.915	1.592
HES68	0.803	0.955	0.158	0.163	1.285	1.719	1.127
HES69	1.331	1.562	0.178	0.226	1.018	1.377	1.280
HES70	0.680	0.967	0.147	0.131	0.676	1.017	0.457
HES71	1.000	1.217	0.182	0.187	0.883	1.354	0.789
HES72	0.341	0.429	0.101	0.079	0.571	0.533	0.408
HES73	1.658	1.846	0.264	0.308	1.136	1.441	1.498
HES74	0.797	0.855	0.086	0.128	0.502	0.659	0.695
HES75	0.139	0.187	-0.001	0.001	0.006	0.056	0.064
HES76	0.302	0.625	0.058	0.053	0.214	0.389	0.196
HES77	0.155	0.248	0.162	0.222	0.067	0.201	0.043
HES78	1.493	1.630	0.159	0.182	0.728	1.122	1.254
HES79	1.909	2.005	0.367	0.369	1.372	1.631	1.854
HES80	0.773	0.720	0.045	0.053	0.455	0.578	0.521
HES81	0.599	0.662	0.097	0.085	0.555	0.680	0.421
HES82	0.657	0.729	0.083	0.077	0.953	1.590	0.806
HES83	0.817	0.759	0.241	0.232	1.107	1.613	1.299
HES84	0.638	0.565	0.015	0.013	0.304	0.365	0.442
HES85	1.960	2.139	0.758	0.731	1.599	2.146	1.849
HES86	0.802	0.771	0.063	0.081	0.996	1.564	0.833
HES87	0.777	1.138	0.158	0.203	1.114	1.751	1.032
HES88	0.600	0.473	0.012	0.012	0.422	0.454	0.386
HES89	0.608	0.657	0.009	0.014	0.794	1.039	0.524
HES90	0.499	0.666	0.008	0.006	0.315	0.448	0.423
HES91	0.678	0.758	0.087	0.056	0.563	0.650	0.395
HES92	0.181	0.290	0.006	0.006	0.129	0.162	0.119
HES93	0.342	0.651	0.201	0.016	0.239	0.355	0.254
HES94	0.398	0.610	0.034	0.026	0.350	0.466	0.268
HES95	0.385	0.653	0.032	0.025	0.220	0.330	0.265
HES96	0.374	0.465	0.035	0.019	0.248	0.577	0.357
HES97	0.237	0.396	0.040	0.021	0.191	0.385	0.188
HES98	0.677	0.873	0.467	0.384	0.314	0.463	0.721
HES99	0.093	0.135	0.023	0.011	0.014	0.008	0.023
HES100	0.215	0.234	0.010	0.003	0.140	0.174	0.073
HES101	0.959	1.068	0.153	0.098	0.531	0.778	0.597
HES102	0.520	0.745	0.099	0.051	0.736	1.071	0.679
HES103	0.343	0.548	0.048	0.014	0.285	0.436	0.332
HES104	0.218	0.393	0.019	0.007	0.329	0.836	0.154
HES105	0.154	0.359	0.013	0.011	0.075	0.138	0.030
HES106	0.517	0.730	0.084	0.066	0.842	1.177	0.731
HES107	0.253	0.462	0.044	0.026	0.582	0.572	0.327
HES108	0.104	0.158	0.002	0.003	0.031	0.091	0.037
HES109	0.021	0.037	-0.001	0.001	-0.001	0.111	0.003
HES110	0.542	0.685	0.067	0.037	0.270	0.350	0.293
HES111	2.146	2.177	0.624	0.587	1.781	2.177	1.840

*RPMI-8226(3) and RPMI-8226(1,2) fixed at different occasion

RPMI-8226 positive in FITC performed at Cellartis

	NCI-H69	NCI-H69 (2)	SK-MES-1	SK-MES-1 (2)	RPMI-8226	RPMI-8226 (2)	RPMI-8226 (3)*
HES112	0.855	1.097	0.248	0.094	0.417	0.655	0.397
HES113	0.750	1.002	0.182	0.122	0.635	0.740	0.656
HES114	0.704	1.015	0.116	0.087	0.316	0.608	0.395
HES115	0.473	0.745	0.079	0.056	0.206	0.287	0.224
HES116	0.327	0.384	0.037	0.015	0.196	0.234	0.224
HES117	0.801	1.083	0.123	0.108	0.394	0.595	0.362
HES118	0.212	0.339	0.014	0.019	0.385	0.873	0.180
HES119	1.437	1.676	0.199	0.210	0.824	1.229	1.453
HES120	0.032	0.051	0.000	0.001	-0.002	-0.005	0.002
HES121	2.114	1.417	0.338	0.081	1.342	1.266	2.357
HES122	0.174	0.236	0.005	0.005	0.056	0.063	0.017
HES123	0.577	0.816	0.211	0.096	0.598	1.003	0.557
HES124	1.289	1.583	0.164	0.137	0.791	1.151	1.360
HES125	2.061	1.440	0.334	0.103	1.357	1.509	2.331
HES126	0.359	0.547	0.037	0.017	0.286	0.456	0.203
HES127	0.148	0.309	0.026	0.006	0.058	0.102	0.038
HES128	0.219	0.252	0.005	0.003	0.094	0.149	0.148
HES129	0.158	0.283	0.015	0.008	0.057	0.109	0.049
HES130	0.241	0.378	0.010	0.004	0.127	0.297	0.213
HES131	0.326	0.644	0.046	0.057	0.163	0.461	0.250
HES132	1.797	1.793	0.724	0.693	1.326	1.716	1.711
HES133	0.726	0.646	0.078	0.051	1.356	1.384	0.815
HES134	0.673	0.815	0.141	0.091	1.212	1.523	0.882
HES135	0.328	0.542	0.048	0.035	0.249	0.319	0.175
HES136	1.133	1.424	0.429	0.424	1.094	1.708	1.253
HES137	1.664	2.157	0.561	0.713	1.488	1.995	1.624
HES138	1.023	1.107	0.080	0.047	0.473	0.702	0.978
HES139	0.858	1.196	0.238	0.197	0.943	1.307	0.784
HES140	0.976	1.305	0.224	0.171	1.060	1.568	1.067
HES141	1.026	1.293	0.177	0.154	1.061	1.681	1.211
HES142	1.555	1.887	0.855	0.803	1.410	1.825	1.512
HES143	1.084	1.097	0.416	0.340	1.058	1.532	1.152
HES144	1.235	1.351	0.180	0.075	1.802	2.164	1.386
HES145	0.851	0.903	0.748	0.570	0.840	1.079	1.038
HES146	1.252	1.437	0.239	0.170	1.616	1.967	1.180
HES147	1.826	2.272	0.926	0.637	1.278	1.713	1.965
HES148	1.461	1.551	0.205	0.158	0.677	1.054	1.460
HES149	1.130	1.307	0.225	0.178	1.388	1.749	1.463
HES150	0.238	0.326	0.061	0.018	0.238	0.418	0.341
HES151	0.934	1.116	0.128	0.103	1.039	1.500	1.210
HEP1	0.547	0.502	0.128	0.085	0.508	0.708	0.562
HEP2	0.770	1.068	0.198	0.220	0.619	1.264	0.661
HEP3	0.310	0.395	0.035	0.030	0.235	0.423	0.294
HEP4	0.926	1.131	0.036	0.022	0.237	0.228	0.071
HEP6	1.317	1.360	0.160	0.094	0.239	0.251	0.107
HEP9	0.361	0.363	0.084	0.075	0.240	0.298	0.160
HEP19	0.714	0.887	0.165	0.103	1.004	1.695	0.943
HEP22	1.330	1.486	0.237	0.269	1.132	1.718	1.174
HEP25	0.991	0.837	0.564	0.497	0.863	1.037	0.758
HEP26	0.353	0.327	0.060	0.012	0.295	0.181	0.216
HEP27	0.620	0.792	0.121	0.078	0.656	1.017	0.480
HEP29	0.158	0.204	0.028	0.025	0.006	0.068	0.030
HEP31	0.278	0.439	0.059	0.028	0.372	0.475	0.233
HEP32	0.118	0.116	0.004	0.003	0.019	0.112	0.023
HEP34	0.824	0.877	0.022	0.026	0.135	0.203	0.033
HEP35	0.497	0.433	0.045	0.050	0.361	0.384	0.221
EB2	0.524	0.588	0.062	0.047	0.322	0.271	0.135

*RPMI-8226(3) and RPMI-8226(1,2) fixed at different occasion RPMI-8226 positive in FITC performed at Cellartis

	NCI-H69	NCI-H69 (2)	SK-MES-1	SK-MES-1 (2)	RPMI-8226	RPMI-8226 (2)	RPMI-8226 (3)
EB7	1.665	1.829	0.464	0.564	1.393	2.061	1.533
EB8	0.984	1.135	0.136	0.086	1.235	1.803	1.062
EB10	2.001	2.264	0.704	0.836	1.709	2.634	2.011
EB12	0.579	0.548	0.131	0.063	0.350	0.645	0.417
EB14	1.159	1.389	0.193	0.150	1.118	1.884	1.377
EB22	0.576	0.582	0.011	0.006	0.053	0.178	0.086
EB23	1.183	1.147	0.187	0.139	1.198	1.471	1.099
EB24	1.058	0.973	0.142	0.118	1.034	1.487	1.257
EB26	1.410	1.458	0.106	0.138	1.017	1.528	1.198
EB30	1.330	1.295	0.167	0.116	0.980	1.547	1.052
EB32	1.599	1.531	0.234	0.165	1.304	1.691	1.375
EB33	0.668	0.627	0.011	0.011	0.049	0.126	0.037
HF1	0.342	0.258	0.253	0.207	0.075	0.411	0.117
HF2	0.137	0.187	0.006	0.005	0.039	0.099	0.026
HF3	0.804	0.805	0.120	0.096	0.813	1.228	0.676
HF4	0.452	0.600	0.027	0.057	0.293	0.359	0.153
HF5	0.762	0.957	0.385	0.336	0.584	0.709	0.647
HF6	0.101	0.102	0.010	0.003	0.029	0.091	0.017
HF7	0.113	0.071	0.456	0.386	0.011	0.035	0.015
HF8	1.472	1.673	0.286	0.210	1.223	1.694	1.373
HF10	1.563	1.434	0.523	0.379	1.220	1.680	1.475
HF11	0.765	1.210	0.138	0.109	0.366	0.437	0.287
HF12	0.139	0.540	0.034	0.024	0.087	0.486	0.047
HF14	0.835	1.246	0.069	0.080	0.330	0.430	0.232

*RPMI-8226(3) and RPMI-8226(1,2) fixed at different occasion RPMI-8226 positive in FITC performed at Cellartis

11.3 Appendix C

11.3.1 CELISA complete results of Colo205, Panc-1, ZR75-1 and NCI-H128

	Colo205	Colo205 (2)	Panc1	Panc1 (2)	ZR75-1	ZR75-1 (2)*	NCI-H128	NCI-H128 (2)
HES89**	0.006	0.005	0.034	0.011	0.033	0.035	0.031	0.047
HES90	0.001	0.004	0.095	0.036	0.040	0.012	0.012	0.014
HES91	0.047	0.027	0.108	0.060	0.029	0.081	0.042	0.017
HES92	0.004	0.005	0.019	0.023	0.029	-0.005	0.004	0.006
HES93	0.005	0.000	0.037	0.040	0.056	0.035	0.035	0.013
HES94	0.002	0.013	0.061	0.094	0.025	0.045	0.010	0.013
HES95	0.003	0.000	0.078	0.079	0.026	0.008	0.010	0.010
HES96	0.005	0.031	0.020	0.058	0.024	0.024	0.034	0.065
HES97	0.009	0.016	0.016	0.077	0.014	0.041	0.016	0.012
HES98	0.009	0.016	0.334	0.280	0.252	0.072	0.182	0.112
HES99	0.002	0.000	0.003	0.030	0.020	0.046	0.007	0.005
HES100	0.003	-0.004	0.023	0.022	0.014	0.031	0.002	0.007
HES101	0.073	0.037	0.138	0.232	0.132	0.184	0.089	0.113
HES102	0.100	0.124	0.129	0.093	0.038	0.274	0.090	0.201
HES103	0.003	0.353	0.026	0.031	0.022	0.126	0.003	0.013
HES104	0.005	0.008	0.027	0.054	0.006	0.013	0.003	0.029
HES105	0.027	0.027	0.034	0.032	0.041	0.013	0.001	0.008
HES106	0.439	0.416	0.093	0.155	0.074	0.501	0.604	0.398
HES107	0.009	0.068	0.042	0.120	0.031	0.125	0.013	0.275
HES108	0.001	-0.002	0.015	0.049	0.009	-0.001	-0.001	0.000
HES109	0.001	-0.003	0.009	0.023	-0.005	0.064	-0.001	0.005
HES110	0.004	0.007	0.053	0.131	0.029	0.074	0.011	0.017
HES111	1.169	1.107	0.738	0.731	0.751	1.620	1.415	1.631
HES112	0.020	0.014	0.193	0.108	0.116	0.518	0.023	0.010
HES113	0.045	0.030	0.217	0.274	0.056	0.159	0.018	0.052
HES114	0.024	0.018	0.172	0.092	0.073	0.084	0.014	0.007
HES115	0.004	0.003	0.173	0.127	0.031	0.060	0.013	0.007
HES116	0.001	0.003	0.084	0.090	0.067	0.043	0.008	0.012
HES117	0.022	0.024	0.123	0.163	0.077	0.075	0.010	0.005
HES118	0.003	0.028	0.048	0.066	0.007	0.015	0.012	0.011
HES119	0.192	0.545	0.206	0.324	0.276	0.869	0.929	1.167
HES120	0.002	-0.003	0.003	0.026	-0.007	-0.005	-0.002	0.002
HES121	1.403	0.578	0.212	0.185	0.282	0.848	1.549	1.032
HES122	0.002	-0.002	0.041	0.032	0.029	0.077	0.009	0.007
HES123	0.222	0.257	0.240	0.136	0.135	0.473	0.076	0.222
HES124	0.241	0.336	0.223	0.155	0.082	0.908	0.872	1.274
HES125	1.567	0.706	0.398	0.143	0.302	0.964	1.117	1.020
HES126	0.011	0.007	0.139	0.070	0.014	0.319	0.002	0.006
HES127	0.005	0.015	0.038	0.084	0.019	0.024	0.003	0.011
HES128	0.005	0.019	0.034	0.048	0.007	0.077	0.020	0.087
HES129	0.003	0.003	0.079	0.083	0.021	0.029	0.003	0.016
HES130	0.002	-0.002	0.036	0.046	0.008	0.003	0.003	0.015
HES131	0.001	0.027	0.052	0.117	0.011	0.140	0.002	0.137
HES132	0.813	0.879	0.577	0.801	0.974	1.227	1.232	1.353
HES133	0.462	0.335	0.142	0.116	0.058	0.723	0.332	0.716
HES134	0.423	0.219	0.144	0.116	0.070	0.458	0.205	0.175
HES135	0.010	0.175	0.083	0.055	0.023	0.047	0.014	0.018
HES136	0.765	0.710	0.391	0.395	0.332	1.251	0.900	0.987
HES137	0.957	1.052	0.764	0.674	0.717	1.545	1.062	1.528
HES138	0.028	0.050	0.175	0.197	0.095	0.465	0.471	0.760
HES139	0.130	0.197	0.224	0.325	0.196	0.572	0.210	0.298

*fixed applying PLL

RPMI-8226 positive in FITC performed at Cellartis

**HES1-88 already tested by project supervisor Karin Majnesjö

	Colo205	Colo205 (2)	Panc1	Panc1 (2)	ZR75-1	ZR75-1 (2)*	NCI-H128	NCI-H128 (2)
HES140	0.536	0.641	0.284	0.322	0.283	0.842	0.818	0.855
HES141	0.468	0.629	0.245	0.319	0.139	0.786	0.861	0.941
HES142	0.726	0.849	0.666	0.902	1.046	1.185	1.279	1.252
HES143	0.540	0.667	0.281	0.540	0.344	0.843	0.972	0.937
HES144	0.504	0.580	0.137	0.127	0.089	0.995	0.802	1.118
HES145	0.393	0.342	0.655	0.501	0.373	0.674	0.309	0.661
HES146	0.698	0.486	0.292	0.267	0.070	0.928	0.439	0.608
HES147	0.243	0.214	0.710	0.504	0.383	0.871	0.534	0.989
HES148	0.140	0.372	0.360	0.299	0.315	0.991	1.011	1.533
HES149	0.553	0.907	0.229	0.288	0.183	1.127	0.970	1.338
HES150	0.010	0.027	0.032	0.063	0.045	0.080	0.084	0.206
HES151	0.253	0.449	0.114	0.181	0.090	0.759	0.643	0.630
HEP1	0.071	0.029	0.149	0.243	0.069	0.093	0.068	0.048
HEP2	0.397	0.664	0.204	0.415	0.134	0.415	0.226	0.319
HEP3	0.033	0.015	0.029	0.095	0.036	0.103	0.074	0.075
HEP4	0.298	0.206	0.314	0.140	0.078	0.488	0.045	0.026
HEP6	0.406	0.380	0.312	0.270	0.137	0.969	0.061	0.040
HEP9	0.004	0.001	0.322	0.374	0.051	0.107	0.011	0.014
HEP19	0.239	0.248	0.171	0.191	0.089	0.624	0.383	0.614
HEP22	0.909	0.735	0.287	0.301	0.154	0.996	0.872	1.096
HEP25	0.078	0.066	0.589	0.668	0.103	0.387	0.113	0.218
HEP26	0.347	0.037	0.216	0.142	0.038	0.043	0.148	0.042
HEP27	0.132	0.136	0.060	0.180	0.021	0.310	0.017	0.094
HEP29	0.037	0.018	0.049	0.150	0.035	0.110	0.012	0.008
HEP31	0.001	0.001	0.034	0.098	0.040	0.036	0.023	0.023
HEP32	-0.001	-0.004	0.002	0.055	0.002	0.003	-0.001	0.007
HEP34	0.211	0.206	0.167	0.190	0.124	0.924	0.025	0.014
HEP35	0.001	-0.009	0.344	0.343	0.095	0.088	0.039	0.019
EB2	0.151	0.135	0.177	0.130	0.080	0.351	0.030	0.013
EB7	0.974	0.948	0.587	0.642	0.524	1.410	1.079	1.259
EB8	0.262	0.602	0.155	0.087	0.041	0.603	0.154	0.374
EB10	0.967	1.342	0.979	0.970	0.812	1.597	1.305	1.535
EB12	0.037	0.031	0.291	0.352	0.051	0.149	0.164	0.183
EB14	0.317	0.524	0.169	0.219	0.208	0.799	0.686	1.072
EB22	0.006	0.011	0.067	0.067	0.063	0.020	0.263	0.246
EB23	0.476	0.394	0.174	0.253	0.153	0.632	0.602	0.516
EB24	0.471	0.915	0.115	0.188	0.197	1.211	0.869	1.089
EB26	0.546	0.729	0.230	0.139	0.121	0.680	0.819	0.806
EB30	0.601	0.592	0.204	0.199	0.074	0.663	0.538	0.573
EB32	0.774	0.660	0.315	0.231	0.141	0.769	0.830	0.922
EB33	0.005	0.013	0.057	0.048	0.024	0.016	0.148	0.217
HF1	0.003	0.000	0.309	0.291	0.167	0.061	0.004	0.039
HF2	0.004	0.002	0.062	0.012	0.019	0.003	0.006	0.006
HF3	0.258	0.293	0.249	0.140	0.074	0.510	0.318	0.351
HF4	0.001	0.008	0.086	0.060	0.007	0.019	0.006	0.005
HF5	0.109	0.189	0.367	0.287	0.461	0.280	0.317	0.320
HF6	0.009	0.005	0.017	0.004	0.002	-0.006	0.002	0.004
HF7	0.002	-0.001	0.523	0.586	0.003	-0.006	0.001	0.001
HF8	0.718	0.680	0.353	0.318	0.205	0.933	0.531	0.951
HF10	0.533	0.710	0.577	0.551	0.421	1.229	0.521	1.089
HF11	0.248	0.218	0.314	0.266	0.050	0.358	0.012	0.035
HF12	0.039	0.026	0.056	0.094	0.004	0.332	0.003	0.019
HF14	0.210	0.236	0.275	0.267	0.056	0.536	0.025	0.011

*fixed applying PLL

RPMI-8226 positive in FITC performed at Cellartis

11.4 Appendix D

11.4.1 CELISA complete results of A427, A549, Calu-3 and SK-MES-1

	A427	A549	Calu-3	SK-MES-1	A549*
HES120	0.092	-0.002	-0.007	0.001	0.015
HES109	0.001	-0.001	-0.002	0	0.061
HES19	0.007	0.001	-0.004	0.001	0.09
HES53	0.007	0.037	0.114	0.01	0.084
HES17	0.024	0.06	0.32	0.142	0.18
HES21	0.021	0.026	0.001	0.004	0.063
HES27	0.019	0.012	0.005	0.005	0.065
HF7	0.014	0.047	0.002	0.526	0.061
HES122	0.049	0.021	0.011	0.003	0.069
HF6	0.195	0.382	0.167	0.015	0.125
HES5	0.016	0.037	0.052	0.01	0.116
HES99	0.022	0.023	0.329	0.011	0.074
HEP32	0.011	0	-0.003	0.001	0.066
HF2	0.014	0.017	0.003	0.001	0.064
HES4	0.026	0.013	0.007	0.006	0.066
HES105	0.045	0.119	0.145	0.039	0.228
HEP29	0.134	0.085	0.09	0.056	0.098
HEP34	0.07	0.085	0.162	0.052	0.147
HES52	0.017	0.033	0.023	0.006	0.355
HES108	0.053	0.032	0.023	0.016	0.172
EB33	0.341	0.047	0.084	0.008	0.085
HES127	0.166	0.288	0.124	0.039	0.141
HES6	0.063	0.41	0.4	0.017	0.789
HES77	0.067	0.191	0.366	0.055	0.078
HES48	0.086	0.001	-0.003	0.006	0.089
HF12	0.111	0.038	0.022	0.036	0.264
HES129	0.053	0.011	0.018	0.038	0.088
HES1	0.061	0.018	0.021	0.02	0.113
HES75	0.006	0.02	0.018	0.002	0.07
HES2	0.102	0.135	0.027	0.134	0.165
HEP4	0.092	0.05	0.192	0.066	0.193
HES100	0.057	0.059	0.028	0.032	0.094
HES37	0.037	0.037	0.014	0.017	0.155
HES58	0.12	0.106	0.097	0.052	0.117
HES34	0.035	0.023	0.028	0.009	0.076
HES41	0.039	0.025	0.058	0.015	0.172
EB22	0.332	0.023	0.051	0.009	0.151
HEP6	0.217	0.124	0.429	0.109	0.365
HF1	0.166	0.177	0.065	0.091	0.153
HES92	0.042	0.058	0.02	0.024	0.104
HES30	0.193	0.036	0.067	0.062	0.48
HES3	0.168	0.256	0.177	0.107	0.19
EB2	0.18	0.092	0.19	0.096	0.162
HES128	0.046	0.043	0.017	0.008	0.063
HF4	0.103	0.114	0.051	0.066	0.148
HES104	0.113	0.157	0.077	0.06	0.233
HES22	0.087	0.075	0.028	0.085	0.149
HEP9	0.094	0.404	0.053	0.101	0.368
HES16	0.078	0.113	-0.005	0.008	0.317
HES135	0.092	0.03	0.025	0.021	0.109
HES118	0.051	0.007	0.016	0.025	0.274

***fixed applying PLL** RPMI-8226 positive in FITC performed at Cellartis

	A427	A549	Calu-3	SK-MES-1	A549*
HES11	0.174	0.251	0.096	0.144	0.488
HES97	0.077	0.059	0.018	0.026	0.271
HES45	0.051	0.017	0.014	0.017	0.106
HES76	0.061	0.037	0.06	0.031	0.094
HES126	0.048	0.057	0.039	0.02	0.209
HES50	0.034	0.095	0.039	0.034	0.189
HES38	0.097	0.095	0.077	0.054	0.445
HES130	0.024	0.025	0.007	0.012	0.143
HEP26	0.065	0.069	0.025	0.009	0.144
HEP35	0.105	0.276	0.011	0.067	0.401
HES115	0.095	0.045	0.037	0.142	0.157
HES116	0.067	0.008	0.02	0.046	0.111
HES33	0.108	0.136	0.042	0.027	0.189
HES35	0.109	0.049	0.018	0.045	0.207
HF14	0.074	0.051	0.105	0.048	0.176
HES49	0.207	0.086	0.121	0.159	0.199
HEP31	0.065	0.044	0.035	0.051	0.163
HES39	0.047	0.05	0.055	0.011	0.244
HES131	0.145	0.132	0.08	0.101	0.306

*****fixed applying PLL RPMI-8226 positive in FITC performed at Cellartis

11.5 Appendix E

11.5.1 ICC summary of results

	A549	A427	Calu-3	SK-MES-1	NCI-H69	NCI-H345	NCI-H128	Panc-1	ZR75-1	Colo205	RPMI-8226
HES6	-	-	+	-	++	+	+	-	n/a	+++	-
HES17	+,membrane	-	++,membrane	++,membrane	-	(+)	-	-	-	-	-
HES53	-	-	++,membrane	++,membrane	-	+++,membrane	-	-	-	+,membrane	-
HES77	-	-	++,membrane	-	-	-	(+)	-	-	-	-
HES99	-	-	++,membrane	-	-	-	+	-	-	-	-
HES105	++, membrane	-	++,membrane	+,(membrane)	-	++,membrane	-	-	n/a	++,membrane	-
HES127	-	-	+	+++,(membrane)	-	++,membrane	-	-	-	+	-
HEP4	++	+	++	+,granula	+,granula	+,granula	(+),granula	+++,membrane	++,membrane	++,membrane	-
HEP6	++	+	++,membrane	+	+,granula	+,granula	+	++,membrane	++,membrane	++,membrane	-
HEP34	+	+	++,membrane	+,granula	+,granula	+,granula	-	++,membrane	++,membrane	++,membrane	-
EB2	+	+	+	-	(+)	(+)	(+)	+,membrane	++, membrane	+,membrane	-
EB22	-	++,membrane	-	-	+++,membrane	(+)	++	-	+++,membrane	-	-
EB33	-	++,membrane	-	-	++,membrane	(+)	++,(membrane)	++,granula	+++,membrane	-	-
HF7	n/a	n/a	n/a	++,membrane	n/a	n/a	n/a	-	-	n/a	-
HES2	n/a	n/a	n/a	++,membrane	++,membrane	n/a	n/a	n/a	n/a	n/a	++,membrane
HES3	+++,membrane	n/a	n/a	n/a	+++,membrane	n/a	n/a	n/a	n/a	n/a	++,membrane
HES131	+,(membrane)	n/a	n/a	n/a	++, membrane	n/a	n/a	n/a	n/a	n/a	+++,membrane
HES11	-	n/a	n/a	n/a	n/a	-	n/a	n/a	n/a	n/a	-
HES58	-	n/a	n/a	n/a	-	n/a	n/a	n/a	n/a	n/a	-
HES104	-	n/a	n/a	n/a	-	n/a	n/a	n/a	n/a	n/a	-
HES115	n/a	n/a	n/a	n/a	-	n/a	n/a	-	n/a	n/a	(+)
HEP9	-	n/a	n/a	n/a	-	n/a	n/a	n/a	n/a	n/a	-
HEP35	-	n/a	n/a	n/a	-	n/a	n/a	n/a	n/a	n/a	-

Results explanation, (): possible signal, +: weak positive, ++: strong positive, +++: very strong positive